

CHALMERS



Design of a broadband antenna element for LTE base station antennas

Master of Science Thesis

MARIE STRÖM

Department of Signals and Systems
Division of Signal Processing and Antennas
CHALMERS UNIVERSITY OF TECHNOLOGY
Göteborg, Sweden, 2009
Report No. EX059/2009

Prepared (also subject responsible if other) EAB/FJN/AA Marie Ström		No. EAB/FJN-09:0218 Uen		
Approved EAB/FJN/A [Stefan Johansson]	Checked	Date 2009-07-02	Rev A	Reference

Design of a broadband antenna element for LTE base station antennas

Master of Science Thesis at the Department of Signals and Systems

Chalmers University of Technology

Conducted at Ericsson AB, FJN/AA, 2009

Marie Ström

Prepared (also subject responsible if other) EAB/FJN/AA Marie Ström		No. EAB/FJN-09:0218 Uen		
Approved EAB/FJN/A [Stefan Johansson]	Checked	Date 2009-07-02	Rev A	Reference

Design of a broadband antenna element for LTE base station antennas

MARIE L. C. STRÖM, 2009

Department of Signals and Systems

Chalmers University of Technology

SE-412 96 Göteborg

Sweden

Telephone + 46 (0)31-772 1000

Prepared (also subject responsible if other) EAB/FJN/AA Marie Ström		No. EAB/FJN-09:0218 Uen		
Approved EAB/FJN/A [Stefan Johansson]	Checked	Date 2009-07-02	Rev A	Reference

Abstract

This report proposes a dual polarized antenna element fed by a Marchand balun, which operates in the 1710-2690 MHz frequency band. This band covers the high band frequencies for the new Long Term Evolution (LTE) system and the current mobile communication systems, 2G and 3G. The complete design of a printed dipole and a bowtie antenna is documented in a comprehensively manner. The analysis of the antennas was performed numerically using the commercial Finite Element Method (FEM) software, Ansoft High Frequency Structure Simulator (HFSS). The optimization of the Marchand balun was performed in Agilent Advance Design System (ADS). The proposed printed dipole antenna with a parasitic element, possesses an operating bandwidth of at least 47%, a +/- 45 degree linear polarization and desirable radiation pattern. A prototype of a designed antenna was built and experimentally validated, producing results that agree with the simulation result.

Keywords: broadband antenna, dipole, Marchand balun, dual polarization

Prepared (also subject responsible if other) EAB/FJN/AA Marie Ström		No. EAB/FJN-09:0218 Uen		
Approved EAB/FJN/A [Stefan Johansson]	Checked	Date 2009-07-02	Rev A	Reference

Acknowledgements

The thesis work has taken place at Ericsson AB, at the department FJN/AA. I would like to express my gratitude to all of the employees at FJN/AA; Anders Ek, Bo Granstam, Henrik Hallenberg, Ola Kaspersson, Håkan Karlsson, Ingolf Larsson and Lars Torstensson for their assistance in technical issues and mainly for making me feel welcome. Thanks to Anders Stjernman and Andreas Nilsson, for assistance with the simulation program HFSS. Foremost, I owe thanks to my supervisor, Henrik Jidhage, for making sure that I was on the right track and answering all of my questions. Also, to the head of department, Stefan Johansson, for giving me this opportunity and making me part of the group.

Finally, thanks to my examiner, Professor Per-Simon Kildahl at the Department of Signals and Systems, Chalmers, for taking time to help me both with technical and administrative issues.

Prepared (also subject responsible if other) EAB/FJN/AA Marie Ström		No. EAB/FJN-09:0218 Uen		
Approved EAB/FJN/A [Stefan Johansson]	Checked	Date 2009-07-02	Rev A	Reference

Abbreviations

ADS	Agilent Advance Design System
CPS	CoPlanar Stripline
FEM	Finite Element Method
HFSS	Ansoft High Frequency Structure Simulator
HGP	Height to Ground Plane
LTE	Long Term Evolution
QN	Quasi Newton
SNLP	Sequential Non-Linear Programming

Prepared (also subject responsible if other) EAB/FJN/AA Marie Ström		No. EAB/FJN-09:0218 Uen		
Approved EAB/FJN/A [Stefan Johansson]	Checked	Date 2009-07-02	Rev A	Reference

Contents

1 Introduction 7

1.1 Purpose..... 7

1.2 Limitations 8

2 Technical requirements and overview..... 9

2.1 Impedance 9

2.2 Frequency band 9

2.3 Return loss 10

2.4 Horizontal 3dB beamwidth..... 10

2.5 Polarization 10

2.6 Mechanical dimensions 10

3 Literature study 11

3.1 Dipole concepts..... 12

3.2 Microstrip antennas 13

3.3 Concept selection..... 13

4 Theory 15

4.1 Dipoles 15

4.1.1 Broadband dipoles 16

4.2 Balun design 16

4.2.1 Marchand balun..... 16

4.3 Impedance matching 17

4.3.1 Quarter-wave transformer 18

4.3.2 Stub-matching 18

4.4 Polarization 18

5 Antenna structure and simulation result..... 19

5.1 Balun design 20

5.1.1 Design procedure for the Marchand balun..... 21

5.2 Dipole concept investigation 22

5.2.1 Printed dipole 23

5.2.2 Bowtie antenna..... 25

5.2.3 Printed dipole with a parasitic element 28

5.2.4 Bowtie with a parasitic element 30

5.2.5 Bowtie with a parasitic element and a tuning slot..... 32

5.2.6 Summary..... 34

5.3 Detailed analysis for the bowtie antenna 35

5.4 Detailed analysis for the printed dipole 39

5.4.1 Removing the parasitic element 44

6 Prototype manufacturing and measurements 45

6.1 Comparison between measurements and simulations..... 47

7 Discussion..... 49

8 Conclusions 50

9 Proposed future work..... 51

10 References 52

Prepared (also subject responsible if other) EAB/FJN/AA Marie Ström		No. EAB/FJN-09:0218 Uen		
Approved EAB/FJN/A [Stefan Johansson]	Checked	Date 2009-07-02	Rev A	Reference

1 Introduction

This report examines the possibility of developing a broadband antenna element for base station antenna applications, which operates in the 1710-2690 MHz frequency band. This band covers the high band frequencies for the current 2G and 3G system, as well as the requirements for the coming LTE system. An important factor considered is the mechanical dimensions; it is important that the antenna can fit in a base station antenna array. To reduce cost and space, the antenna should be dual polarized to support polarization diversity instead of space diversity. Other important characteristics for the antenna are low return loss and proper radiation pattern. The investigation aims to evaluate solutions for designing a broadband antenna, with an emphasis on accomplishing dual polarization in combination with a desirable return loss.

Different antenna solutions are investigated, to establish which accomplishes the broadband characteristics and the other specific requirements (described in section 2). In section 3, a short introduction to different antenna concepts, including the findings from the literature study on investigated antennas, is presented. A brief theory behind dipoles, baluns and matching techniques relevant for this project can be found in section 4. Section 5 shows the complete design for a printed dipole and a bowtie antenna in the simulation program HFSS. The design process is described in a comprehensive manner from the basic structure to the final version of the antenna. The results, including impedance matching, radiation properties, beamwidth and polarization are included in the design process. Section 6 discusses the manufacturing of a prototype for a designed antenna. Simulations carried out are presented and compared with the results of physical testing of the antenna. This is followed by a discussion, conclusions and suggestions for future improvements.

1.1 Purpose

Nowadays, the market demand for wireless communication systems is growing rapidly. The development of mobile broadband systems requires higher data rate to satisfy the customer demand. In order to meet these demands, the new LTE system has started to be introduced to the market. The LTE system will provide a higher data rate, lower delay, improved coverage and spectral efficiency compared to the 3G system. The current mobile communication systems, 2G and 3G, are already fully established on the market. When implementing the new LTE system, it is necessary to ensure compatibility between it and the existing systems, as the LTE technique is introduced successively.

One way for the systems to co-exist could be to mount an extra LTE antenna on the site. However, this can be difficult due to the limited site space and increased site rent. Another solution is to develop a broadband antenna that makes it possible for the systems to share the same antenna. The possibility for such a solution is examined in this report. Another positive factor is a reduction in the number of possible product variants.

Prepared (also subject responsible if other) EAB/FJN/AA Marie Ström		No. EAB/FJN-09:0218 Uen		
Approved EAB/FJN/A [Stefan Johansson]	Checked	Date 2009-07-02	Rev A	Reference

1.2 Limitations

For an antenna to function properly, the radiation properties for both the co-polarization and cross-polarization need to be evaluated. The cross-polarization is always undesirable and should be much lower than the maximum gain of the co-polarization. Back radiation is also undesirable and should be as low as possible. In this report, only a small amount of attention is given to analyze the cross-polarization and back radiation.

Prepared (also subject responsible if other) EAB/FJN/AA Marie Ström		No. EAB/FJN-09:0218 Uen		
Approved EAB/FJN/A [Stefan Johansson]	Checked	Date 2009-07-02	Rev A	Reference

2 Technical requirements and overview

The requirements for a base station antenna element operating in the LTE and 3G systems can be seen in Table 1. The limitations for the parameters are set so that the antenna element can operate in an antenna array.

Parameter	Requirement
Impedance	50 Ω
Frequency band	1710 - 2690 MHz
Return loss	>15 dB
Horizontal 3dB beamwidth	60 – 70°
Polarization	+/- 45°
Mechanical dimensions	
– Element separation	<105 mm
– Element height	<50 mm

Table 1: Project requirements.

2.1 Impedance

The antenna will be connected to a 50 Ω coaxial cable. It is therefore important for the antenna element to be matched to an input impedance of 50 Ω .

2.2 Frequency band

The frequency band 1710 to 2690 MHz includes the current 2G, 3G and the standard for the next generation of wireless mobile system, LTE. In this frequency range, the return loss criterion is 15dB.

The broad frequency spectrum requires a high fractional bandwidth, calculated to 45 % with Eq. 1 ($f_H = 2690$, $f_L = 1710$ and $f_0 = 2200$ MHz).

$$fb = \frac{f_H - f_L}{f_0} \quad \text{Eq. 1}$$

Prepared (also subject responsible if other) EAB/FJN/AA Marie Ström		No. EAB/FJN-09:0218 Uen		
Approved EAB/FJN/A [Stefan Johansson]	Checked	Date 2009-07-02	Rev A	Reference

2.3 Return loss

There is a need for a low return loss to ensure low losses in the antenna system. The return loss coefficient [Eq. 2] is defined as the amount of relative power from the source that is reflected in the system towards the load.

$$RL_{DB} = -10 \log_{10} \frac{P_R}{P_T} \quad \text{Eq. 2}$$

2.4 Horizontal 3dB beamwidth

The 3dB beamwidth describes the angular separation between two points in the antenna radiation pattern, where the gain is half of its maximum value.

2.5 Polarization

The polarization of the antenna describes the direction for the transmitted electrical field, and can be linear, circular or elliptical. Here, a +/- 45 degree linearly polarized antenna is required.

2.6 Mechanical dimensions

The antenna is supposed to be used in a base station antenna array; see Figure 1 for a typical layout. Hence, there is a limitation in space. The antennas are spaced with 105mm (center to center), the reflector is 137mm in width and the height is limited to 50mm, to fit inside the cover of the base station.

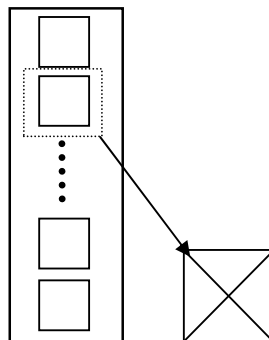


Figure 1: Antenna array in a base station.

Prepared (also subject responsible if other) EAB/FJN/AA Marie Ström		No. EAB/FJN-09:0218 Uen		
Approved EAB/FJN/A [Stefan Johansson]	Checked	Date 2009-07-02	Rev A	Reference

3 Literature study

This section shows the outcome of the literature study. For the literature study, different articles about antennas were investigated. These articles give knowledge about concepts that can accomplish the final layout.

Access to various databases and magazines provided a great amount of information. Interesting scientific articles and conference papers were found in the databases IEEE Xplore [1], Inspec [2] and the online version of Microwave letters. The search was concentrated on articles concerning broadband antenna elements.

There are many different types of antenna elements. Some basic forms are:

- Wire antennas
 - Dipoles
 - Loop antennas
- Aperture antennas
 - Horn antennas
 - Waveguides
- Microstrip antennas
- Array antennas
 - Yagi-Uda arrays
 - Aperture arrays
- Reflector antennas
- Lens antennas

For this project, the wire antenna (especially dipoles) and microstrip antenna are particularly interesting, due to their broadband characteristics, simplicity to manufacture and small dimensions [3]. The abstracts for the articles that are interesting for further work in this project are presented in the following pages.

Prepared (also subject responsible if other) EAB/FJN/AA Marie Ström		No. EAB/FJN-09:0218 Uen		
Approved EAB/FJN/A [Stefan Johansson]	Checked	Date 2009-07-02	Rev A	Reference

3.1 Dipole concepts

A New Quasi-Yagi Bowtie Type Integrated Antenna [4]

“This work presents an optimized broadband quasi-Yagi planar antenna with a new driver configuration that looks like a bowtie antenna for wireless communication applications. The proposed quasi-Yagi antenna represents an improvement over existing printed antenna topologies, simultaneously exhibiting increased bandwidth, excellent radiation properties, and simple design. The antenna was firstly designed to work at 2.4 GHz, satisfying the standards of Bluetooth system and WLAN, and finally was optimized to include the frequency of 1.9 GHz and PCS applications. The simulation and design optimization were done by a commercial software, CST Microwave Studio, that uses the Finite Integration Technique (FIT). Numerical results are compared to measured ones and good agreement is observed.”

A Novel Broadband Printed Dipole Antenna with Low Cross-Polarization [5]

“A novel broadband printed dipole antenna with low cross-polarization is presented. The printed dipole employs a double-layered structure where the E-field component perpendicular to the dipole arms is minimized, thus low cross-polarization is obtained. Measurement results show that the printed dipole antenna achieves a bandwidth up to 50% while reducing the cross-polarization level to less than 30 dB within the frequency band.”

Novel Broadband Printed Dipole [6]

“In this paper, a novel printed antenna is presented, which achieves broadband features through a dipole with parasitic element fed by a new microstrip Balun. Experimental result shows that the impedance bandwidth is 49.5% for VSWR ≤ 1.5 , and the cross polarization level is better than ≤ 21 dB over the entire frequency band, and it should find wide application in radar and wireless communication systems.”

A CPW-Fed Bow-Tie Antenna with Tuning Stub [7]

“In this paper, a modified slot bow-tie antenna fed by a coplanar waveguide (CPW) is investigated for wideband operation. It is designed to work on a thin substrate ($h = 0.787\text{mm}$) with a low dielectric constant $\epsilon_r = 2.2$ operating at two frequencies (1.8 and 2.4 GHz). Two metal stubs are introduced in the middle of the bow-tie slot in order to achieve a wider impedance bandwidth over the conventional CPW-fed bow-tie slot antenna. The antenna is fabricated and tested in the antenna measurement facility of UCL and experimental far-field results are presented showing low cross-polarisation levels. The bow-tie slot antenna can obtain at least 55% bandwidth.”

Novel E-Shaped Driver based on the Quasi-Yagi Antenna [8]

“Telecommunication devices are getting smaller and smaller, thus size of antenna which is the heart of the communication must be small too. Microstrip antenna was developed to fit this criterion. In this paper, a new E-shaped Driver based on the Quasi-Yagi Antenna is presented. This microstrip antenna is realized on a dielectric-constant substrate with $\epsilon_r = 4.4$. Size of the new proposed design is only 70 mm in width, 80 mm in length and 1.62 mm in thickness. Operating frequency runs from 1.6 GHz to 3.1 GHz which covers many applications such as mobile phone, WLAN, Bluetooth, and 3G.”

Prepared (also subject responsible if other) EAB/FJN/AA Marie Ström		No. EAB/FJN-09:0218 Uen		
Approved EAB/FJN/A [Stefan Johansson]	Checked	Date 2009-07-02	Rev A	Reference

3.2 Microstrip antennas

Analysis of Stacked V-slot Loaded Patch Antenna for Wideband Application [9]

“The analysis of V-slot loaded antenna stacked with simple patch is carried out using equivalent circuit model. It is found that stacked patch antenna exhibits enhanced bandwidth that depends on various dimensions of the V-slot. The proposed theoretical results are compared with simulated and reported experimental results which are in good agreement.”

Dual Polarized Wide-Band Aperture Stacked Patch Antennas [10]

“A wide-band, dual polarized printed antenna is designed and developed in this paper. The antenna is based upon an aperture stacked patch layout and incorporates a simple dual-layered feeding technique to achieve dual-polarized radiation. The printed antenna has a measured 10 dB return loss bandwidth of 52% and an isolation between the excitation ports of greater than 39 dB over this frequency range. The gain of the antenna is 7.4 dBi 0.4 dB and the typical issues associated with incorporating an aperture excited solution are resolved by using a cross-shaped reflector patch to ensure the front-to-back ratio is greater than 20 dB.”

Wideband Dual-Polarized Patch Antenna With Broadband Baluns [11]

“A pair of novel 180 broadband microstrip baluns are used to feed a dual-polarized patch antenna. The 180 broadband balun delivers equal amplitude power division and consistent 180(5) phase shifting over a wide bandwidth (50%). We demonstrate that for a dual-polarized quadruple L-probe square patch antenna, the use of the proposed 180 broadband balun pair, in place of a conventional 180 narrowband balun pair, provides improved input port isolation and reduced H-plane cross-polarization levels over a wider frequency range, while maintaining low E-plane cross-polarization levels and stable E- and H-plane co-polarization patterns throughout the impedance passband.”

3.3 Concept selection

Several antenna concepts were investigated, although none fulfill the requirements completely. Patch antennas are a good choice when requirements such as a low-cost, low-profile and simplicity to add a dual polarization are important. However, a major disadvantage for the patch antennas is that they have a too narrow bandwidth (as in article [9], [10] and [11]) for a 15dB return loss criterion. Considering the dipole concepts, the modified bowtie antenna and the printed dipole appear to satisfy the requirements for this project. For the bowtie, the reason behind the choice is mainly the broadband characteristics and the low cross-polarization levels. In addition, another important attribute is the simple structure that makes it easy to design and manufacture. However, the printed dipole has an even simpler structure and similar broadband characteristics.

Prepared (also subject responsible if other) EAB/FJN/AA Marie Ström		No. EAB/FJN-09:0218 Uen		
Approved EAB/FJN/A [Stefan Johansson]	Checked	Date 2009-07-02	Rev A	Reference

To increase the impedance bandwidth, the effect of adding a parasitic element as described in article [4] and [8] is evaluated through simulations. Another way to improve the characteristics of the antenna could be to add a tuning stub as described in article [7]. A tuning stub may also decrease the size of the radiator due to the fact that the stub increases the electrical length of the antenna.

All of the articles about dipoles found in the literature study investigate a single polarized element. In this project, a dual polarized antenna is essential. Hence, two similar antennas are developed and mounted together as a cross. This is described in section 4.1.

To design the matching network for the antenna, the Marchand balun described in section 4.2.1 is proposed due to its simple structure and the fact that it can be printed directly on the substrate.

Prepared (also subject responsible if other) EAB/FJN/AA Marie Ström		No. EAB/FJN-09:0218 Uen		
Approved EAB/FJN/A [Stefan Johansson]	Checked	Date 2009-07-02	Rev A	Reference

4 Theory

In this section, a brief introduction to dipoles, baluns, impedance matching techniques and polarization is given.

4.1 Dipoles

The dipole is, if considered in the simplest case, a two-wire transmission line as shown in Figure 2a. The transmission line is driven by a signal source in one end and an open circuit on the other side. The result of the open circuit is a standing wave on the transmission line. The current at the edges is zero due to a phase shift created in the source. This results in a zero net radiation. Thus, to design a radiating element, the two edges are turned to create the simple wire dipole sketched in Figure 2b. This modification radiates due to the fact that the currents now have the same orientation in space [12]. The current distribution depends on the length L for the dipole. In practice, the most common way is to choose the length to half or a quarter of a wavelength. The radiation resistance for the half wavelength dipole is 73Ω [3].

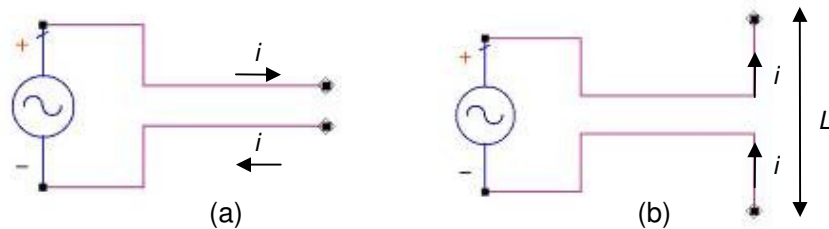


Figure 2: (a) Two-wire transmission line, (b) A simple wire dipole

A requirement for this project is to examine a dual polarized antenna; the dipole element is a single polarized element. To achieve dual polarization, it is possible to design two dipole elements and mount them as a cross, or to design one dipole and mount it four times in a square. In Figure 3, the two different possibilities are illustrated.

Prepared (also subject responsible if other) EAB/FJN/AA Marie Ström		No. EAB/FJN-09:0218 Uen		
Approved EAB/FJN/A [Stefan Johansson]	Checked	Date 2009-07-02	Rev A	Reference

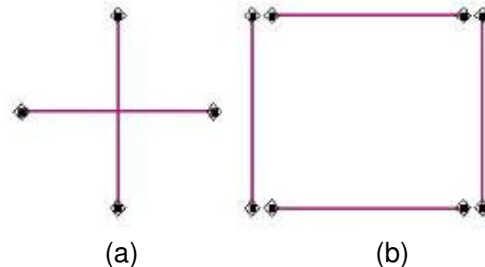


Figure 3: Solutions to achieve quad polarization, (a) Two dipoles in a cross, (b) Four dipoles in a square.

If the dipole element is connected to an unbalanced source, for example a coaxial cable, it is necessary to implement a balun to create the 180° phase shift needed at the radiator. The design of a balun is described in section 4.2.

4.1.1 Broadband dipoles

In order to reach the required bandwidth, a dipole with broadband characteristics is required. There are numerous ways for designing such an antenna. For example: dipole arrays, biconical and cylindrical dipoles can all achieve broadband characteristics. However, dipole arrays have large physical dimensions, and considering the requirement for a small structure, a biconical dipole antenna could be a better choice. Furthermore, the design of a biconical antenna is impractical due to the fact that the shell structure is massive [3]. Instead, an approximation of the biconical antenna, namely a bowtie type antenna, is interesting.

4.2 Balun design

For a dipole element to radiate, it needs to be fed by a balanced source. A balun is a three port network that couples the unbalanced source at one port to a balanced load at the other two ports. Moreover, the balun can perform impedance matching. There are different types of baluns, for example: Bazooka balun, Coaxial balun and Marchand balun. In this project, the Marchand balun is proposed and described in the next section.

4.2.1 Marchand balun

The Marchand balun is used for its compact size, broadband characteristics, simplicity to print on a substrate and ease of fabrication. The Marchand balun can be designed in four different ways, see Figure 4, depending on the amount of freedom degrees needed.

Prepared (also subject responsible if other) EAB/FJN/AA Marie Ström		No. EAB/FJN-09:0218 Uen		
Approved EAB/FJN/A [Stefan Johansson]	Checked	Date 2009-07-02	Rev A	Reference

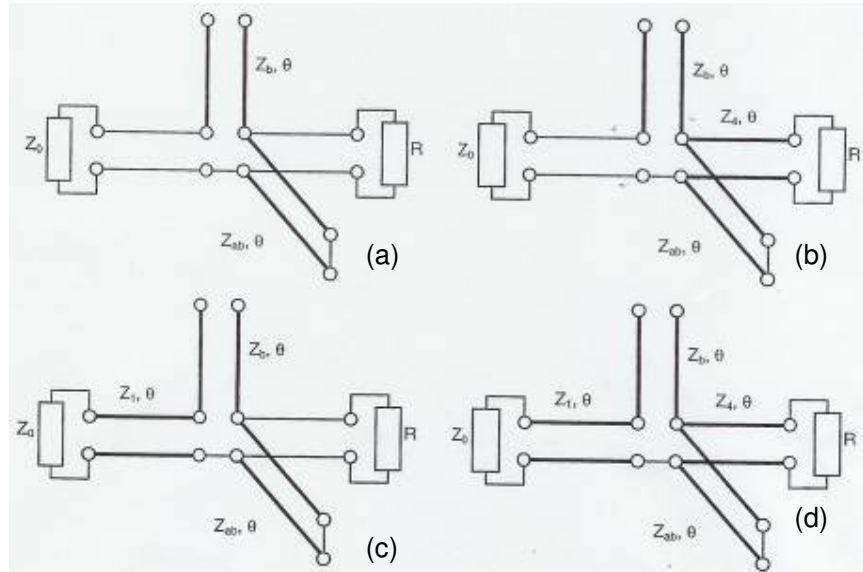


Figure 13. Marchand balun (a), second order (b), third order (c), fourth order [13].

The second order balun consists of a short circuit and an open circuit with impedances Z_{ab} and Z_b respectively, and electrical length of θ degrees. For the third and fourth order balun, transmission lines are connected to the source and the load. To realise the balun, the transmission lines are implemented as microstrip lines and CoPlanar Striplines (CPS), (see Appendix A, for formulas describing the fourth order Marchand balun).

4.3 Impedance matching

To achieve a maximum power transfer the system needs to be matched with the correct impedances. The frequency response for the antenna is not only dependent on the characteristics of the antenna; it also depends on the characteristics of the transmission lines. Therefore, an efficient matching between the transmission lines and the antenna radiator over the desired frequency range is needed. The Smith chart is the most common tool to analyze and design high frequency circuits. From the Smith chart, it is easy to convert the load impedance to a reflection coefficient. The reflection coefficient is calculated with Eq. 3 and describes the power transfer of the circuit [14].

$$\Gamma = \frac{Z_L - Z_S}{Z_L + Z_S} \tag{Eq. 3}$$

Matching techniques, such as the quarter-wave transformer and stub-matching are explained in the following sections.

Prepared (also subject responsible if other) EAB/FJN/AA Marie Ström		No. EAB/FJN-09:0218 Uen		
Approved EAB/FJN/A [Stefan Johansson]	Checked	Date 2009-07-02	Rev A	Reference

4.3.1 Quarter-wave transformer

A method for matching two impedances with each other is to add a single-series transmission line. The quarter-wave transformer is a common tool when matching real impedances. Eq. 4 describes the characteristic impedance that matches the source impedance Z_S to the load impedance Z_L [15].

$$Z_T = \sqrt{Z_S Z_L} \quad \text{Eq. 4}$$

4.3.2 Stub-matching

Another method for matching impedances is to add an open or shorted stub. The stub is positioned somewhere along the transmission line connected to the load and can produce an imaginary impedance. The choice between using an open or shorted stub depends on the type of transmission line used, described by Prof. Grosch in [15] as: *“An open stub is preferred when using microstrip lines because shorted lines are more difficult to fabricate. Shorted stubs are preferred when using coaxial cable because the coaxial short circuits are more perfect than the open circuits”*. For this project, both an open and a shorted stub is used.

4.4 Polarization

At a given point in space, the time-varying characteristic of the electrical field for a wave, describes the polarization of the wave. If the behavior for the radiated wave is observed in the far field, the field can locally be regarded as a propagating plane wave [16]. There are three different classes of polarization: circular, elliptical or linear. The polarization is linear if the electric field as a function of time is directed along a line. This is accomplished if there is only one component or two orthogonal linear components that have a mutual time-phase difference of $n\pi$ (where $n = 0, 1\dots$) [1]. The two components of the electrical field (E_x, E_y) that describe the polarization can be modulated with different signals at the same frequency. Hence, it is possible to re-use the frequencies.

In order to gain performance using polarization, both the transmitter and the receiver antenna must be able to detect the signals with low mutual interference between the signals. Polarization diversity gives a maximum gain when both of the inputs receive radiation in an orthogonal manner with equal field strength. Thus, there is a need for low coupling between the antennas in order to achieve a good impedance matching as well as good radiation performance [11].

To describe the efficiency, both the co-polarization and the cross-polarization need to be evaluated. The cross-polarization is always undesirable and should be much lower than the maximum of the co-polarization. Back radiation is also undesirable and should be as low as possible [3].

Prepared (also subject responsible if other) EAB/FJN/AA Marie Ström		No. EAB/FJN-09:0218 Uen		
Approved EAB/FJN/A [Stefan Johansson]	Checked	Date 2009-07-02	Rev A	Reference

5 Antenna structure and simulation result

This section describes the design process for the printed dipole and the bowtie antenna. The investigation includes impedance matching and radiation pattern evaluation.

Through the literature study and concept selection, the two above mentioned antenna types show desirable impedance matching. The simulation tool Ansoft HFSS (version 11.1) was used to perform the analysis. HFSS uses the FEM to compute the electromagnetic behavior for high frequency components [18].

Both of the antennas require a matching network. The impedances and electrical lengths for the proposed balun are calculated with Agilent ADS [19], an electronic design program where circuit design is easy and parameter optimization is fast. The results from ADS are converted to physical widths and lengths in LineCalc and in the computational program Matlab [20].

Dividing the design process into different steps gives a better insight and control over how the design parameters affect the result. Therefore, that approach is used throughout this section. The design steps are:

- Basic design for the antennas
- Adding a parasitic element
- +/- 45 degrees rotation of the antenna
- Attaching the balun to the antenna
- Mount the second antenna to achieve dual polarization

Both of the different antenna structures are printed on a substrate. As material for the substrate, Taconic RF-30 with a dielectric constant of 3.0 and a loss tangent of 0.0014 is used. Taconic RF-30 is fabricated in two thicknesses, 0.8mm and 1.6mm. In this project, a 0.8mm thick substrate was selected.

To simulate the design in HFSS, a vacuum box with dimension 150x200x200mm covers the structure. To the vacuum box, a radiation boundary that allows waves to radiate infinitely far into space is added. In HFSS the wave is absorbed at this radiation boundary.

For all of the design steps, an impedance matching with a Marchand balun is performed in ADS. This is described in section 5.1.1. The optimization for the balun is done to evaluate the possible matching properties for the antenna. Moreover, after the antennas are mounted together, HFSS is used to do the complete optimization. When using the optimization function in HFSS, there is a possibility to use five different optimizers [18]. Here, two different optimizers were used, the Quasi-Newton (QN) and the Sequential Non-Linear Programming (SNLP) optimizer.

Prepared (also subject responsible if other) EAB/FJN/AA Marie Ström		No. EAB/FJN-09:0218 Uen		
Approved EAB/FJN/A [Stefan Johansson]	Checked	Date 2009-07-02	Rev A	Reference

For the start up the QN optimizer was used. This optimizer took a long time and often resulted in an error message (Out of Memory). In order to speed up the simulations the other optimizer, SNLP was tested with satisfying results. Compared to the QN, the available memory was sufficient to carry out the computations, and it was less time-consuming. Another way to do the optimization is using Matlab to write a script that enables its interoperation with HFSS. This would make the computation time significantly smaller.

To investigate the radiation pattern and 3dB beamwidth, the embedded far field is obtained for the frequencies 1700, 1950, 2200, 2450 and 2690 MHz. The far field data from the HFSS simulations, were exported as a *.csv file, to be analyzed in Matlab. The +/- 45 degree polarization is calculated from the theta and phi components according to the equations defined in Eq.5.

$$\begin{aligned}
 E_{+45^\circ}^{Port_1} &= \frac{1}{\sqrt{2}} (E_{\theta}^{Port_1} + E_{\phi}^{Port_1}) \\
 E_{-45^\circ}^{Port_1} &= \frac{1}{\sqrt{2}} (E_{\theta}^{Port_1} - E_{\phi}^{Port_1}) \\
 E_{+45^\circ}^{Port_2} &= \frac{1}{\sqrt{2}} (E_{\theta}^{Port_2} + E_{\phi}^{Port_2}) \\
 E_{-45^\circ}^{Port_2} &= \frac{1}{\sqrt{2}} (E_{\theta}^{Port_2} - E_{\phi}^{Port_2})
 \end{aligned}
 \tag{Eq.5}$$

5.1 Balun design

The investigated dipoles are fed by an unbalanced microstrip transmission line. A balun is consequently needed to feed the balanced dipoles. A good choice for the matching network is to implement a Marchand balun, which performs the 180 degree phase shift and the impedance matching. Moreover, the balun is printed directly on the substrate and therefore no extra space is required. A Marchand balun with four freedom degrees, as seen in Figure 5, is proposed. The choice is natural, since the electrical length for Z_4 has to be changed when mounting the antennas as a cross. Furthermore, impedance matching can be easier due to the fact that there are more parameters to optimize.

Prepared (also subject responsible if other) EAB/FJN/AA Marie Ström		No. EAB/FJN-09:0218 Uen		
Approved EAB/FJN/A [Stefan Johansson]	Checked	Date 2009-07-02	Rev A	Reference

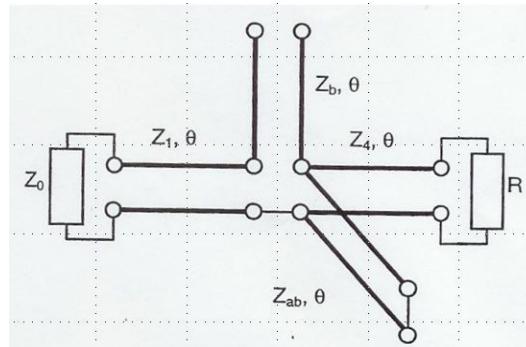


Figure 5: Marchand balun with four freedom degrees [13].

The second order Marchand balun consists of a microstrip line, a CPS and an open ended microstrip line that transforms an unbalanced source to a balanced connection at the load. A third order balun is created by adding an impedance transformer at the input of the balun. Finally, the fourth order balun is created by allowing the excitation point to change in relation to the CPS. The ground plane will act as a return path for the feed connection as well as a reflector for the antenna configuration

5.1.1 Design procedure for the Marchand balun

The design parameters for the balun depend on the frequency behavior of the antenna. The antenna model is simulated in HFSS and the impedance matrix is exported to ADS. The circuit model for a Marchand balun (illustrated in Figure 6), is designed in ADS.

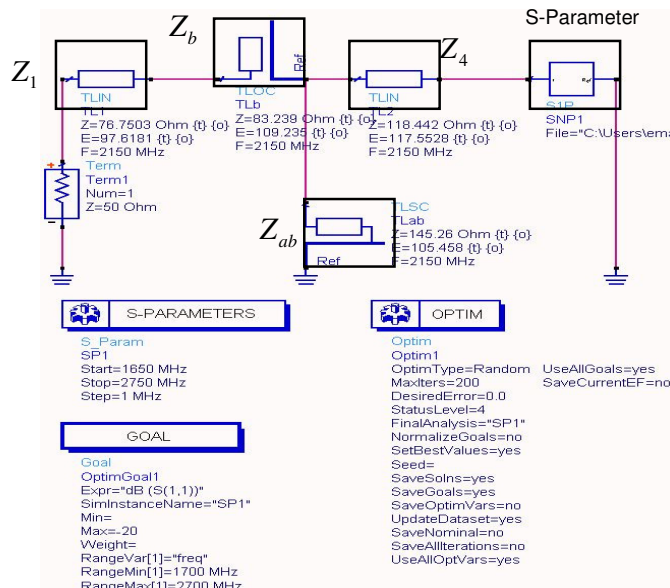


Figure 6: Circuit model for the Marchand balun in ADS.

Prepared (also subject responsible if other) EAB/FJN/AA Marie Ström		No. EAB/FJN-09:0218 Uen		
Approved EAB/FJN/A [Stefan Johansson]	Checked	Date 2009-07-02	Rev A	Reference

With this circuit model, the balun parameters (as the impedances and electrical lengths of the transmission lines), are optimized according to the impedance matrix imported from HFSS. The optimization shows the feasible theoretical matching for the antenna. The impedance and electrical length of the transmission lines are converted to a physical length and width in LineCalc and Matlab. LineCalc is an additional feature in ADS. The balun was implemented in HFSS according to the optimized physical length and width. In HFSS, after a fine adjustment of the balun parameters, the possible impedance matching is similar to the obtained result in ADS. Figure 7 shows the design structure for the balun in HFSS.

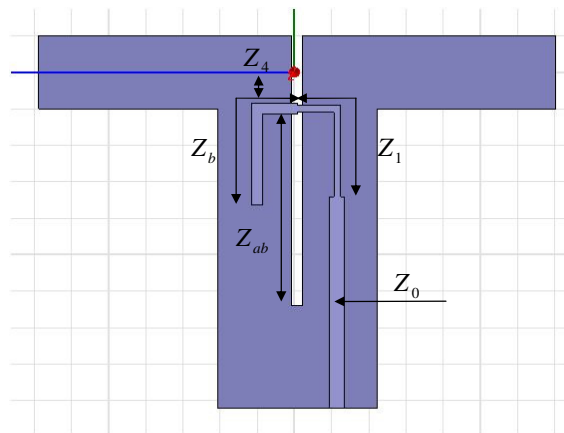


Figure 7: Design of the Marchand balun connected to a dipole radiator in HFSS.

5.2 Dipole concept investigation

In this section, five different concepts focusing on a printed dipole and a bowtie antenna are evaluated. The investigated concepts are:

- Basic design of a printed dipole
- Basic design of a bowtie antenna
- Printed dipole with a parasitic element
- Bowtie with a parasitic element
- Bowtie with a parasitic element and tuning slot

The investigation includes initial HFSS antenna optimization and the theoretical matching with the balun in ADS. The antenna impedance is optimized for 50Ω , a value which is investigated further in section 5.4. The radiation pattern for horizontal polarization is evaluated to ensure proper characteristics. The investigation is followed by a short summary in section 5.2.6.

Prepared (also subject responsible if other) EAB/FJN/AA Marie Ström		No. EAB/FJN-09:0218 Uen		
Approved EAB/FJN/A [Stefan Johansson]	Checked	Date 2009-07-02	Rev A	Reference

5.2.1 Printed dipole

The design parameter definitions for the printed dipole can be seen in Figure 8, and the nominal values are calculated according to:

- L_{Dir} : Half wavelength for the center frequency 2.2 GHz, calculated with Eq. 6 to 38mm ($c = 3 \cdot 10^8$, $\epsilon_r = 3.0$).
- W_{Dir} : Chosen from the width suggested for the design in article [6] to 4.5mm.
- S : Has to be greater than the thickness of the substrate. Here, 1.5mm was chosen.
- HGP : half wavelength, calculated before to 38mm.

$$\lambda = c / \sqrt{\epsilon_r} f \tag{Eq. 6}$$

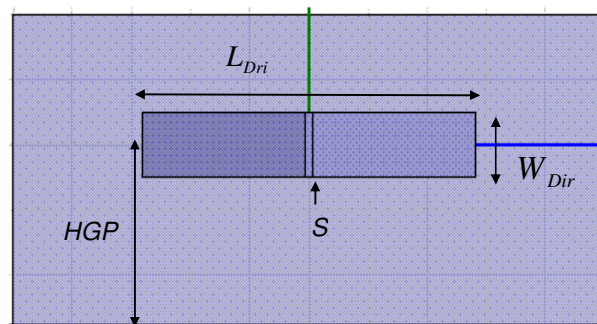


Figure 8: Basic design for the printed dipole radiator.

The parameters were tuned to evaluate how the matching properties are affected. Starting with L_{Dir} and W_{Dir} shown in Figure 9, followed by HGP shown in Figure 10.

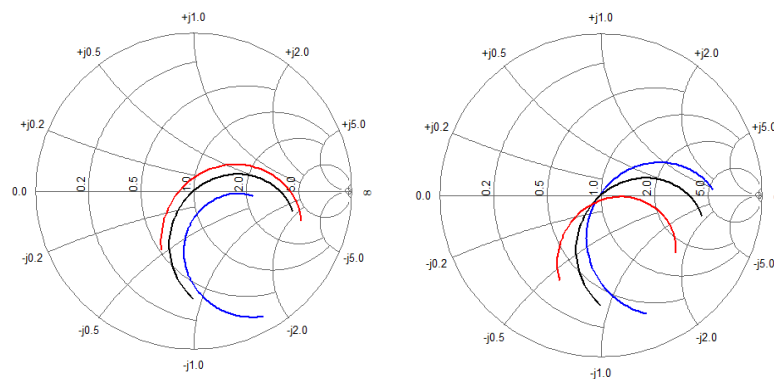


Figure 9: The Smith chart for several lengths (to the left, blue=45mm, black=55mm, red=60mm) and widths (to the right, blue=5mm, black=10mm, red=20mm) for the printed dipole antenna (HGP is fixed to 27.5mm).

Prepared (also subject responsible if other) EAB/FJN/AA Marie Ström		No. EAB/FJN-09:0218 Uen		
Approved EAB/FJN/A [Stefan Johansson]	Checked	Date 2009-07-02	Rev A	Reference

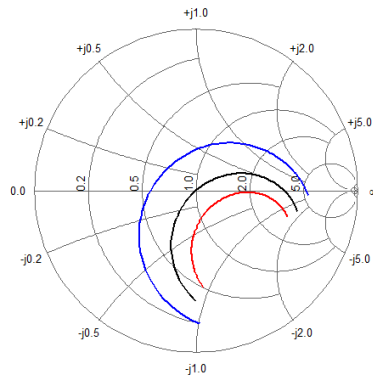


Figure 10: The Smith chart for several HPG (blue=20mm, black=27.5mm, red=34mm) for the printed dipole antenna.

By examination of the Smith charts, it is clear that when using the values: $L_{Dri} = 55\text{mm}$, $W_{Dir} = 10\text{mm}$ and $HPG = 27.5\text{mm}$, a matching close to 50Ω is achieved. To evaluate how well the antenna can be matched, the Marchand balun was optimized according to the S_{11} -parameters. The matching properties can be seen in Figure 11. In the Smith chart, a closed loop is formed centered around the 50Ω point. However, as can be seen in the amplitude plot, the return loss is too high compared with the requirement of 15dB.

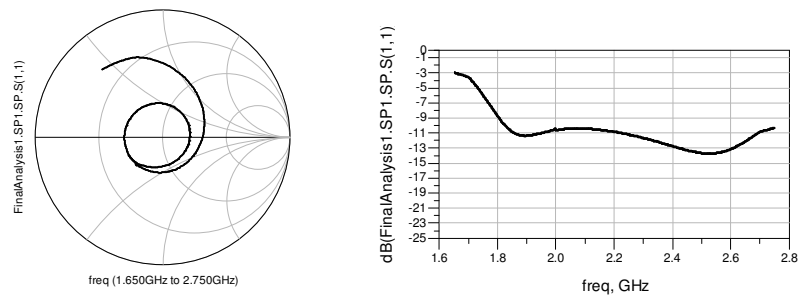


Figure 11: The Smith chart and the amplitude plot for the S_{11} -parameters for the printed dipole antenna optimized with ADS.

In order to obtain the radiation pattern, the theta and phi components for the far field were exported to Matlab, the resulting radiation pattern can be seen Figure 12. Table 2 shows the corresponding 3dB horizontal beamwidth.

Prepared (also subject responsible if other) EAB/FJN/AA Marie Ström		No. EAB/FJN-09:0218 Uen		
Approved EAB/FJN/A [Stefan Johansson]	Checked	Date 2009-07-02	Rev A	Reference

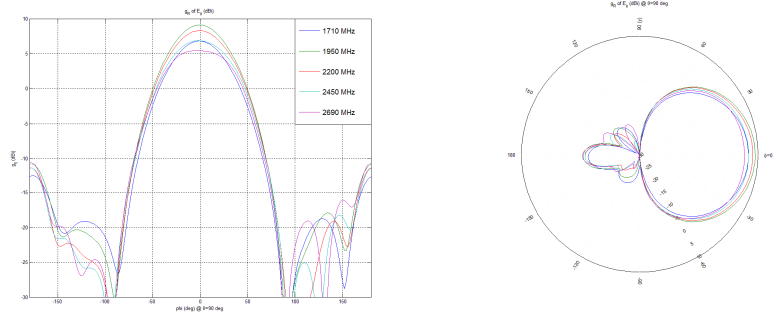


Figure 12: Horizontal radiation pattern ($\theta=90^\circ$) for the printed dipole antenna.

Frequency [MHz]	1710	1950	2200	2450	2690
Beamwidth [Deg]	57	57	59	65	69

Table 2: The 3dB horizontal beamwidth.

5.2.2 Bowtie antenna

The second design evaluated is the bowtie antenna, which is a planar modified biconical antenna. The structure for the bowtie antenna is more complex than for the printed dipole. The design parameters for a basic bowtie antenna are shown in Figure 13, and are calculated in a similar way as for the printed dipole (S and HGP have the same initial values).

- L_{Bow} : Half wavelength for the center frequency 2.2 GHz and calculated with Eq. 6 ($c = 3 \cdot 10^8$ and $\epsilon_r = 3.0$) to 38mm.
- W_{Bow} : Chosen similar to the width of the design in article [4] to 11.5mm.

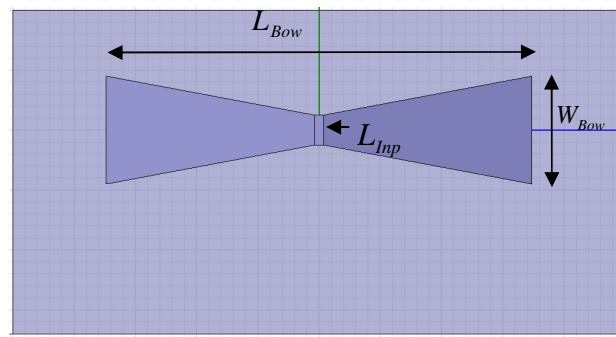


Figure 13: Basic design for the bowtie antenna.

The different parameters were tuned to evaluate the change in matching properties. Starting with L_{Bow} and W_{Bow} (see Figure 14), followed by L_{Inf} and HGP (see Figure 15).

Prepared (also subject responsible if other) EAB/FJN/AA Marie Ström		No. EAB/FJN-09:0218 Uen		
Approved EAB/FJN/A [Stefan Johansson]	Checked	Date 2009-07-02	Rev A	Reference

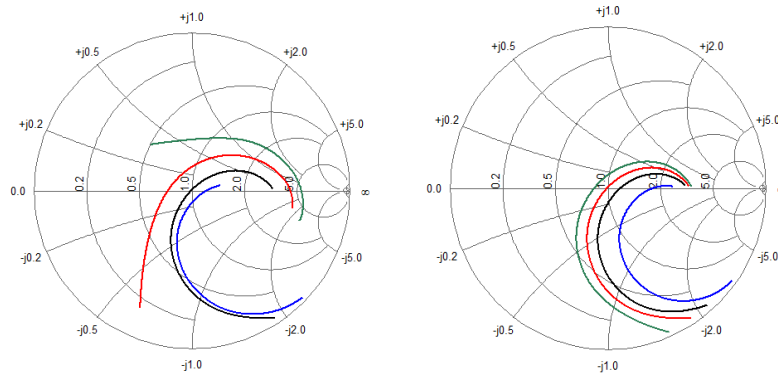


Figure 14: The Smith chart for several lengths (to the left, blue=30mm, black=40mm, red=50mm, green=60mm) and widths (to the right, blue=10mm, black=20mm, red=25mm, green=30mm) for the bowtie antenna.

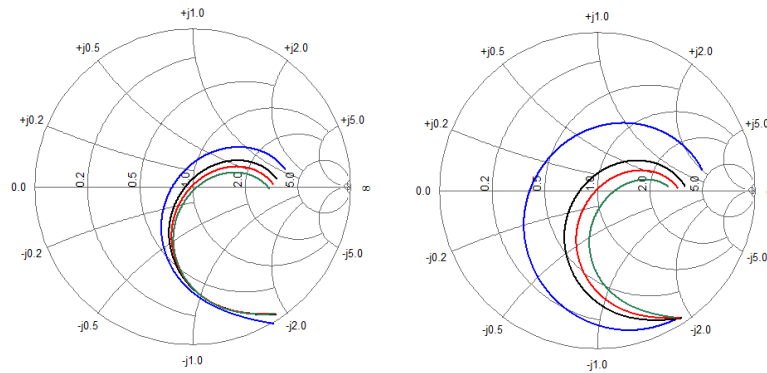


Figure 15: The Smith chart and amplitude plot for several widths of the input (to the left, blue=2mm, black=4mm, red=5mm, green=6mm) and *HGP* (to the right, blue=20mm, black=30mm, red=34mm, green=40mm) for the bowtie antenna.

By examining the Smith charts, it is clear that when using the values: $L_{Bow} = 40\text{mm}$, $W_{Bow} = 25\text{mm}$, $L_{Imp} = 5\text{mm}$ and $HGP = 34\text{mm}$, a matching close to 50Ω is achieved. The S_{11} -parameters were exported to ADS and a Marchand balun was optimized to the frequency behaviour for the antenna. The matching properties can be seen in Figure 16. In the Smith chart, a closed loop is formed centered around the 50Ω point. However, the return loss is too high compared with the goal of 15dB.

Prepared (also subject responsible if other) EAB/FJN/AA Marie Ström		No. EAB/FJN-09:0218 Uen		
Approved EAB/FJN/A [Stefan Johansson]	Checked	Date 2009-07-02	Rev A	Reference

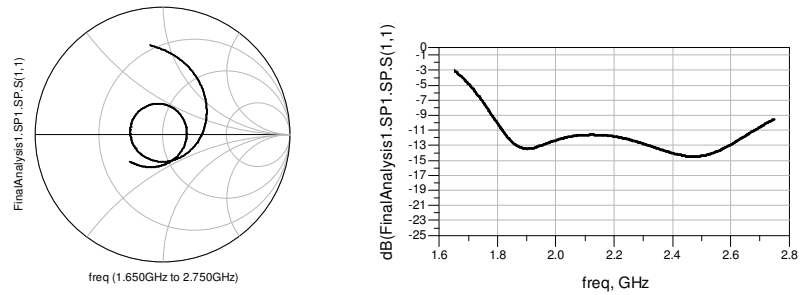


Figure 16: The Smith chart and the amplitude plot for the S_{11} -parameters for the bowtie antenna optimized with ADS.

To ensure proper radiation characteristics, the theta and phi components for the far field were exported to Matlab. Figure 17 shows the radiation pattern, and the corresponding values of the 3dB beamwidth are presented in Table 3. A concern is the ripple of the maximum gain between the frequencies.

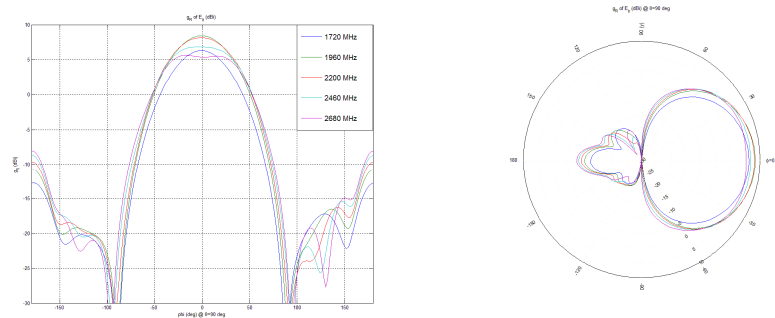


Figure 17: Horizontal radiation pattern ($\theta=90^\circ$) for the bowtie antenna.

Frequency [MHz]	1710	1950	2200	2450	2690
Beamwidth [Deg]	60	62	67	78	79

Table 3: The 3dB horizontal beamwidth.

Prepared (also subject responsible if other) EAB/FJN/AA Marie Ström		No. EAB/FJN-09:0218 Uen		
Approved EAB/FJN/A [Stefan Johansson]	Checked	Date 2009-07-02	Rev A	Reference

5.2.3 Printed dipole with a parasitic element

One way to further increase the bandwidth is to add a parasitic element, as described by article [4] and [6]. The length and width for the parasitic strip are initially similar to those of the design proposed by article [4]. The design structure for the dipole after adding the parasitic element can be seen in Figure 18. The parasite increases the bandwidth by adding an extra resonance to the higher frequencies, as long as the dimensions are chosen properly. To achieve a better matching for the lower frequencies, the length of L_{Dri} was increased. Here, the length of the driver was changed from 50mm to 68mm. Moreover, HPG was increased from 27.5mm to 33mm.

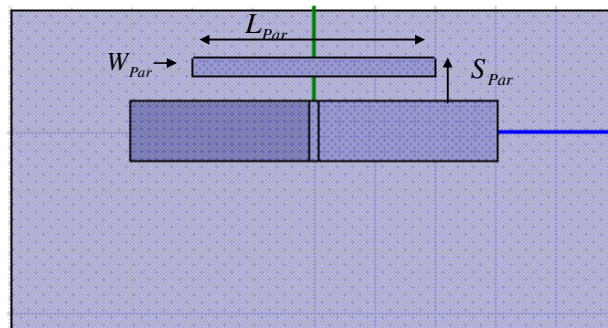


Figure 18: Design of the printed dipole with an additional parasitic element

The parameters for the parasitic element are tuned to achieve the best performance. Figure 19 shows the Smith chart for changes in L_{Par} and S_{Par} , followed by Figure 20 that shows changes for W_{Par} .

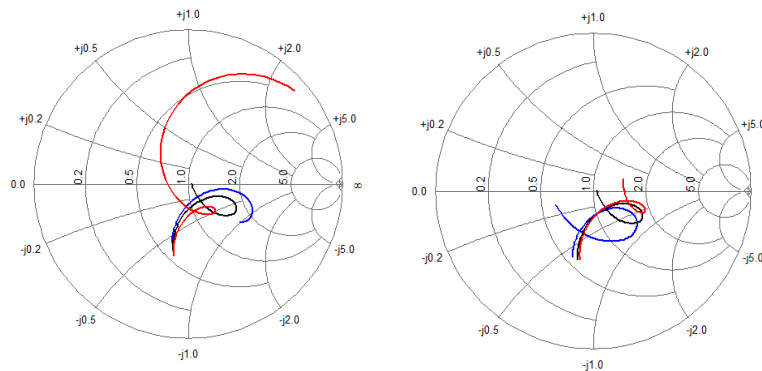


Figure 19: The Smith chart for several lengths for the parasitic element (to the left, blue=35mm, black=40mm, red=45mm) and distances (to the right, blue=5mm, black=7mm, red=9mm) between the dipole and it.

Prepared (also subject responsible if other) EAB/FJN/AA Marie Ström		No. EAB/FJN-09:0218 Uen		
Approved EAB/FJN/A [Stefan Johansson]	Checked	Date 2009-07-02	Rev A	Reference

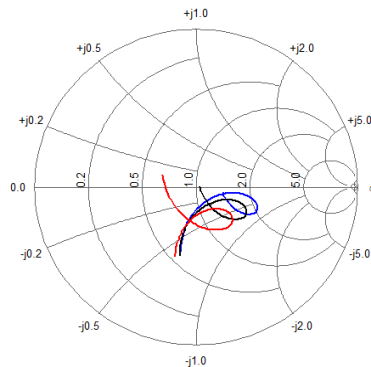


Figure 20: The Smith chart for several widths for the parasitic element (blue=1mm, black=3mm, red=5mm).

As can be seen in the Figure 19 and 20, there is a great advantage when adding a parasitic element. The second resonance gives a better matching for the higher frequencies. The design parameters: $L_{Par} = 40\text{mm}$, $W_{Par} = 3\text{mm}$ and $S_{Par} = 7\text{mm}$, were chosen to accomplish a compact and centered loop in the Smith chart. The S_{11} -parameters were exported to ADS, and a Marchand balun was optimized according to the frequency behavior of the antenna. The result can be seen in Figure 21. A closed and compact loop is formed in the center of the Smith chart. Hence, when adding the parasite, the bandwidth is increased and a theoretical return loss of 15dB is achievable.

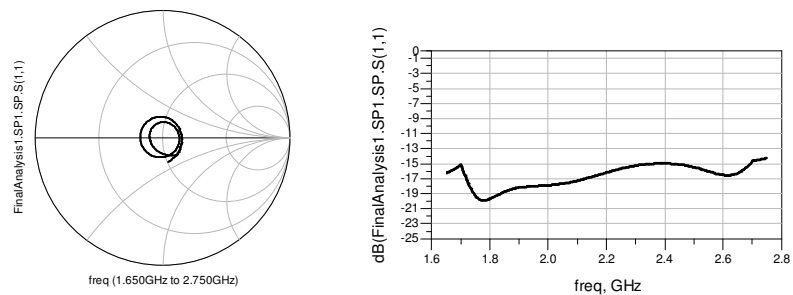


Figure 21: The Smith chart and the amplitude plot for the S_{11} -parameters for the printed dipole with a parasitic element optimized with ADS.

The radiation patterns are calculated in Matlab and shown in Figure 22. The corresponding 3dB beamwidth can be found in Table 4. As can be seen the 3dB beamwidth is increased compared to the design without a parasite. This depends mainly on the fact that the distance between the dipole and ground plane was increased to 33mm.

Prepared (also subject responsible if other) EAB/FJN/AA Marie Ström		No. EAB/FJN-09:0218 Uen		
Approved EAB/FJN/A [Stefan Johansson]	Checked	Date 2009-07-02	Rev A	Reference

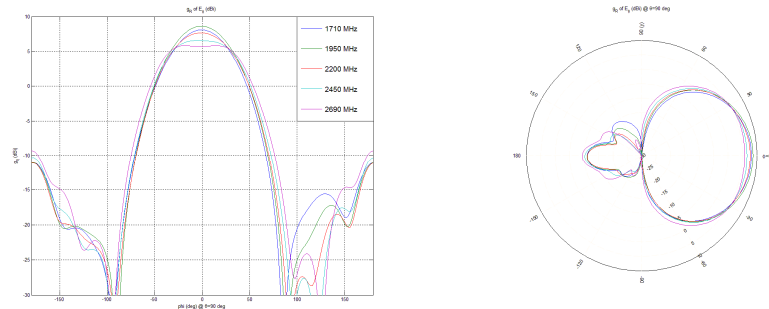


Figure 22: Horizontal radiation pattern ($\theta=90^\circ$) for the printed dipole antenna with a parasitic element.

Frequency [MHz]	1710	1950	2200	2450	2690
Beamwidth [Deg]	59	60	65	73	78

Table 4: The 3dB horizontal beamwidth.

5.2.4 Bowtie with a parasitic element

The proposed structure for the bowtie antenna with a parasitic element can be seen in Figure 23. To give an enhancement for the antenna performance, the parasite needs to be excited. Therefore, the length of the radiator was changed from 40mm to 52mm, the width was decreased from 25mm to 16mm and HGP is 34mm.

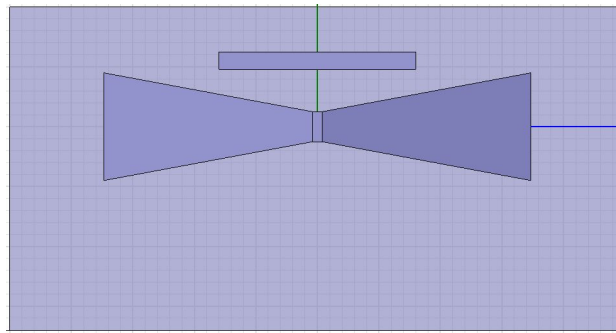


Figure 23: Design for the bowtie antenna with an added parasitic element.

The parameters for the parasite were tuned to evaluate how the matching properties for the antenna are affected. Starting with L_{Par} and S_{Par} (see Figure 24), followed by W_{Par} (see Figure 25).

Prepared (also subject responsible if other) EAB/FJN/AA Marie Ström		No. EAB/FJN-09:0218 Uen		
Approved EAB/FJN/A [Stefan Johansson]	Checked	Date 2009-07-02	Rev A	Reference

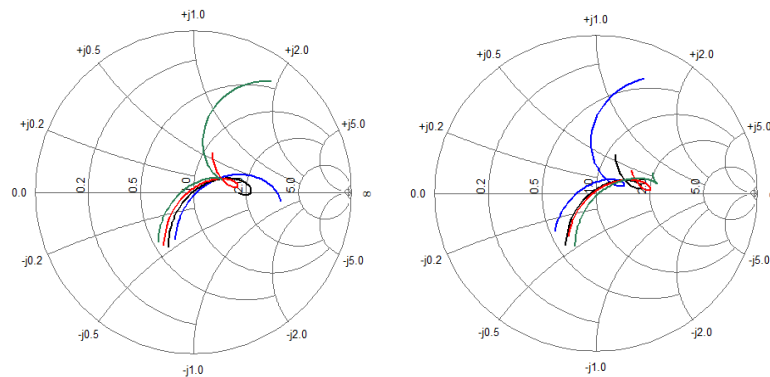


Figure 24: The Smith chart for several lengths of the parasitic element (to the left, blue=25mm, black=35mm, red=37.5mm, green=40mm) and distances (to the right, blue=5mm, black=7mm, red=10mm, green=10mm) between the bowtie and it.

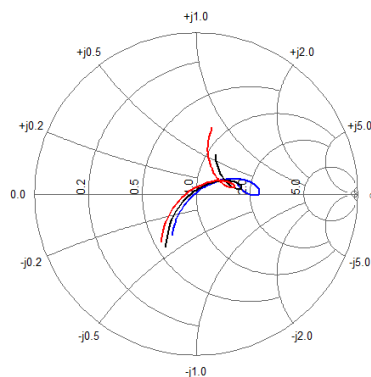


Figure 25: The Smith chart for several widths (blue=0.5mm, black=2mm, red=2.5mm) of the parasitic element.

The advantage of using a parasitic element is clearly shown in the figures. A closed loop is formed in the Smith chart, implying an extra resonant frequency. The dimensions of the parasitic element: $L_{Par} = 37.5\text{mm}$, $W_{Par} = 2\text{mm}$ and $S_{Par} = 7\text{mm}$ were chosen to make the loop in the Smith chart as compact as possible. The Marchand balun was optimized according to the S_{11} -parameters in ADS. The matching properties can be seen in Figure 26. Compared to the result before the parasitic strip was added (shown in Figure 16), the matching properties are enhanced. The return loss is 15 dB for almost the entire frequency spectrum.

Prepared (also subject responsible if other) EAB/FJN/AA Marie Ström		No. EAB/FJN-09:0218 Uen		
Approved EAB/FJN/A [Stefan Johansson]	Checked	Date 2009-07-02	Rev A	Reference

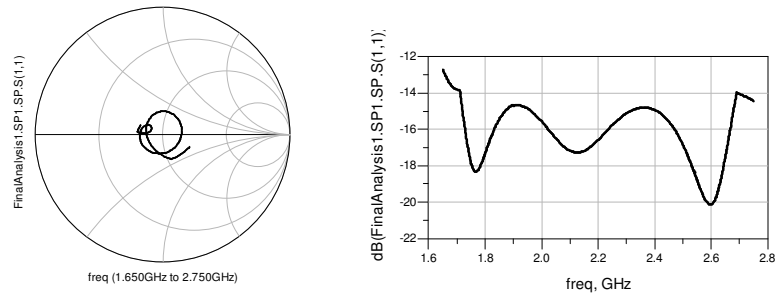


Figure 26: The Smith chart and the amplitude plot for the S_{11} -parameters for the bowtie antenna with a parasitic element optimized with ADS.

The radiation pattern is shown in Figure 27 and the corresponding values of the 3dB beamwidth are presented in Table 5. The difference compared to the previous result is a reduced ripple in the gain for the higher frequencies, and that the 3dB beamwidths are consistently greater.

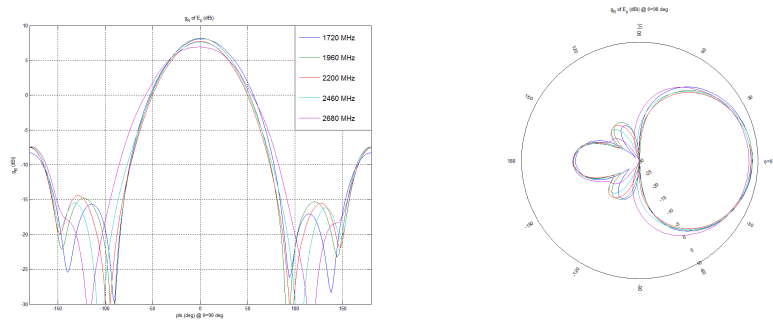


Figure 27: Horizontal radiation pattern ($\theta=90^\circ$) for the bowtie antenna with a parasitic element.

Frequency [MHz]	1710	1950	2200	2450	2690
Beamwidth [Deg]	68	64	63	66	74

Table 5: The 3dB horizontal beamwidth.

5.2.5 Bowtie with a parasitic element and a tuning slot

One way to achieve a wider impedance bandwidth for the bowtie antenna is to add two modified slots, similar to the design in article [7], where instead two stubs are used. A resumé is that “adding the stub increases the input resistance, which results in better matching”. The tuning slot, if correctly added, can increase the electrical length of the antenna, making it possible to decrease the physical length of the radiator. Figure 28 shows the proposed design in which the tuning slots are added in the center outside of the antenna.

Prepared (also subject responsible if other) EAB/FJN/AA Marie Ström		No. EAB/FJN-09:0218 Uen		
Approved EAB/FJN/A [Stefan Johansson]	Checked	Date 2009-07-02	Rev A	Reference

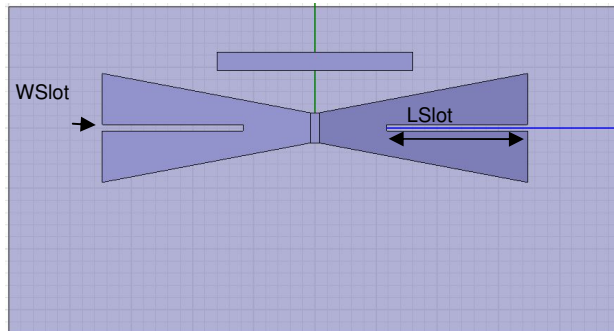


Figure 28: Design for the bowtie antenna with a parasitic element and a tuning slot.

Figure 29 shows the Smith chart after the tuning slot is added to the bowtie structure. As can be seen, adding a short tuning slot gives no difference in the matching properties. However, if the tuning slot has a greater length, two loops are formed in the Smith chart. This could improve the matching properties for the antenna. However, by adding two more parameters, the structure of the antenna becomes more complex and more optimization time is required.

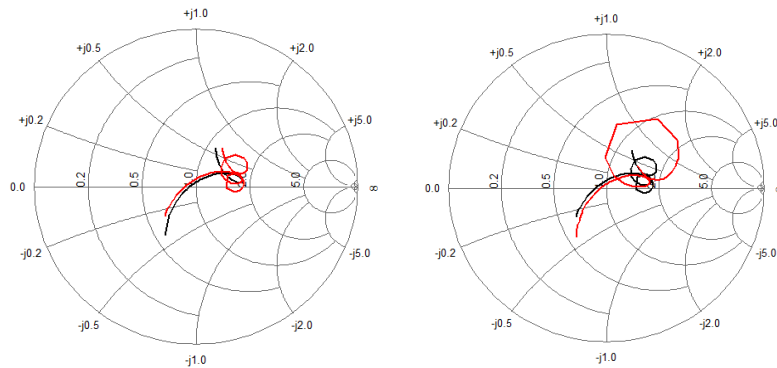


Figure 29: The Smith chart for change of the length (to the left, black=5mm, red=20mm) and change of the width (to the right, black=1mm, red=2mm) for the tuning slot.

If a tuning slot is to be used, the interesting interval of the dimensions are: $1\text{mm} < L_{Slot} < 20\text{mm}$ and $W_{Slot} < 5\text{mm}$. Figure 30 shows the matching properties after the S_{11} -parameters are matched with the Marchand balun. It appears that the impedance matching is worse for the lower frequencies, compared to when a tuning slot is not added. In addition, the impedance matching for the higher frequencies is increased.

Prepared (also subject responsible if other) EAB/FJN/AA Marie Ström		No. EAB/FJN-09:0218 Uen		
Approved EAB/FJN/A [Stefan Johansson]	Checked	Date 2009-07-02	Rev A	Reference

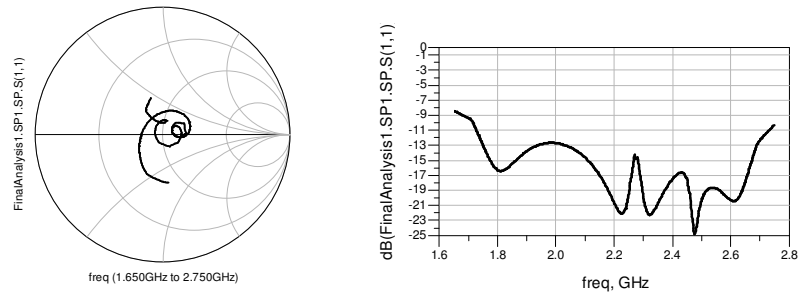


Figure 30: The Smith chart and the amplitude plot for the S_{11} -parameters for the bowtie antenna with a parasitic element and a tuning slot optimized with ADS.

The radiation pattern is shown in Figure 31, and the corresponding values for the 3dB beamwidth are presented in Table 6. The radiation pattern for the higher frequencies has an undesirable appearance, as the tuning slot changes the characteristics drastically. However, by decreasing the length of the slot, a better radiation pattern is achievable, as shown in Figure 31.

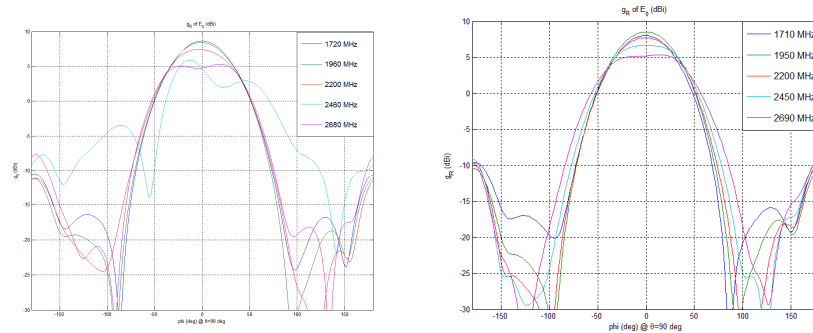


Figure 31: Horizontal radiation pattern ($\theta=90^\circ$) for the bowtie antenna with a parasitic element and a tuning slot.

Frequency [MHz]	1710	1950	2200	2450	2690
Beamwidth [Deg]	60	62	70	-	-

Table 6: The 3dB horizontal beamwidth.

5.2.6 Summary

Through the concept investigation, two designs are interesting for further analysis. The theoretical simulations in ADS show that the printed dipole and the bowtie, both with a parasitic element, can fulfill the requirements in terms of impedance matching. For both designs, a fractional bandwidth of 46% for the return loss criterion 14.5dB is achievable.

Prepared (also subject responsible if other) EAB/FJN/AA Marie Ström		No. EAB/FJN-09:0218 Uen		
Approved EAB/FJN/A [Stefan Johansson]	Checked	Date 2009-07-02	Rev A	Reference

5.3 Detailed analysis for the bowtie antenna

In order to achieve the final design, the antenna is rotated +/- 45 degrees relative to the ground plane. This represents a +/- 45 degree linear polarization. Furthermore, the size of the ground plane is changed to a square with dimensions 137x137mm. The top view for one antenna is illustrated in Figure 32.

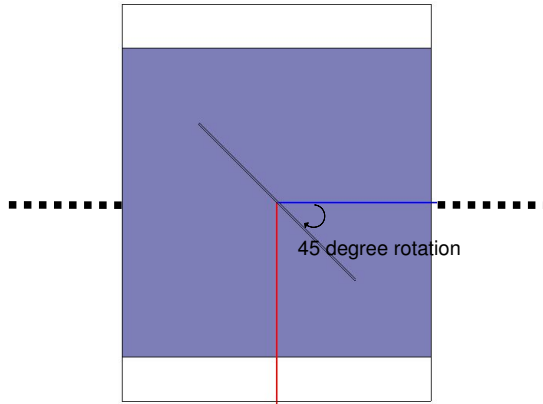


Figure 32: Top view for one rotated antenna.

After these changes were done, the Marchand balun in ADS was optimized to the S_{11} -parameters, exported from HFSS. Notice that, for the CPS, there is a limitation in the physical constraints for the width. Here, the impedance of the CPS was set to 120Ω . Figure 33 shows the matching properties from the theoretical optimization in ADS. The return loss is better than 14dB for all of the frequencies. However, it appears to be difficult to satisfy a 15dB return loss, especially for the lower frequencies. A way to achieve a wider bandwidth could be to increase the *HGP*; though doing so results in a worse radiation pattern (see Appendix B), which is not desirable.

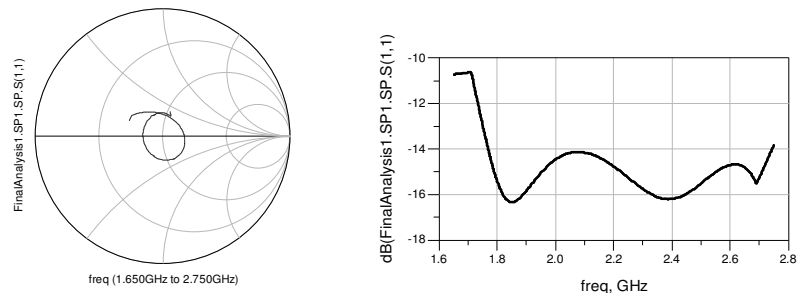


Figure 33: The Smith chart and the amplitude plot for the S_{11} -parameters for the bowtie antenna optimized with ADS.

The optimized impedances and electrical lengths for the transmission lines are shown in Table 7.

Prepared (also subject responsible if other) EAB/FJN/AA Marie Ström		No. EAB/FJN-09:0218 Uen		
Approved EAB/FJN/A [Stefan Johansson]	Checked	Date 2009-07-02	Rev A	Reference

Transmission line	Impedance [Ω]	Electrical length [θ]
Z_1	89	80
Z_b	77	50
Z_4	120	0
Z_{ab}	120	116

Table 7: Calculated impedances and electrical lengths.

The impedances and electrical lengths were transformed to physical lengths and widths (see Table 8), using LineCalc in ADS for the microstrip lines and Matlab for the CPS.

Transmission line	Length [mm]	Width [mm]
Microstripline Z_1	12.5	0.94
Microstripline Z_b	20	0.69
CPS Z_4	0	0
CPS Z_{ab}	38.8	30

Table 8: The physical lengths and widths.

The balun is printed on two sides of the substrate. On one side the bowtie radiator is connected to a shorted CPS. On the opposite side the microstrip lines create the other design of the balun. When designing the balun for the second polarization, Z_4 was tuned down to have a physical length of 5mm. This makes it possible for the antennas to be mounted as a cross with low interference between each other. To compensate for the additional length of Z_4 , the length of Z_{ab} was tuned from 38.8mm to 36mm. The balun is fed by a 50 Ω microstrip line (50 Ω corresponds to a physical width of 2mm). The microstrip line is in turn connected to a wave port, which symbolizes the signal source. To make the correct mode propagate through the wave port, the dimensions of the wave port are of great importance. Here, the dimensions 12x4.8mm give the characteristic field behaviour for a microstrip line and can be seen in Figure 34.

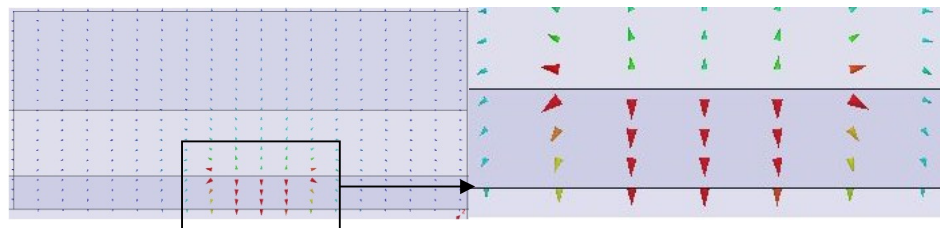


Figure 34: Field lines for a microstrip line fed with a wave port.

Prepared (also subject responsible if other) EAB/FJN/AA Marie Ström		No. EAB/FJN-09:0218 Uen		
Approved EAB/FJN/A [Stefan Johansson]	Checked	Date 2009-07-02	Rev A	Reference

The two bowtie antenna elements are mounted orthogonally with respect to each other, creating a cross as illustrated in Figure 35. When mounting the antennas together, there was no significant change in the matching properties. However, the need to make an extra slot in the ground plane affects the matching characteristics. In order to have a minimal change, the slot is made as thin as possible. A condition that has to be fulfilled is that the space between the ground plane and the microstrip line should be large enough so that an excitation does not occur between them.

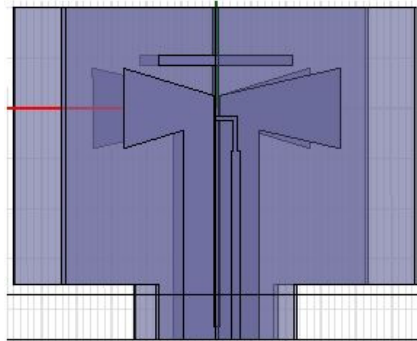


Figure 35: Two bowtie antennas mounted in a cross to create a dual polarized antenna.

Simulations in HFSS show that the calculated widths and lengths of the microstrip lines are consistent with the result obtained in ADS. However, the width of the CPS calculated in Matlab is not consistent with the correct impedance in HFSS. Instead, simulations in HFSS give a width of 21.5mm. The matching properties for the bowtie antenna after an optimization in HFSS can be seen in Figure 36 and in Figure 37, for the frequency range 1500 to 3000 MHz. The fractional bandwidth was calculated to 35% and 32% (see Table 9).

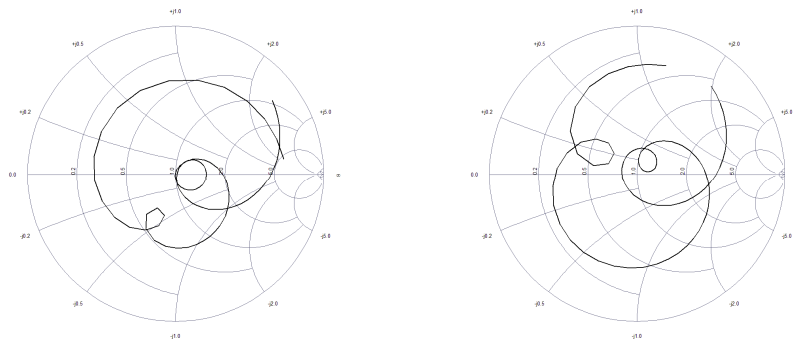


Figure 36: The Smith chart for the first antenna (to the left) and for the second antenna (to the right).

Prepared (also subject responsible if other) EAB/FJN/AA Marie Ström		No. EAB/FJN-09:0218 Uen		
Approved EAB/FJN/A [Stefan Johansson]	Checked	Date 2009-07-02	Rev A	Reference

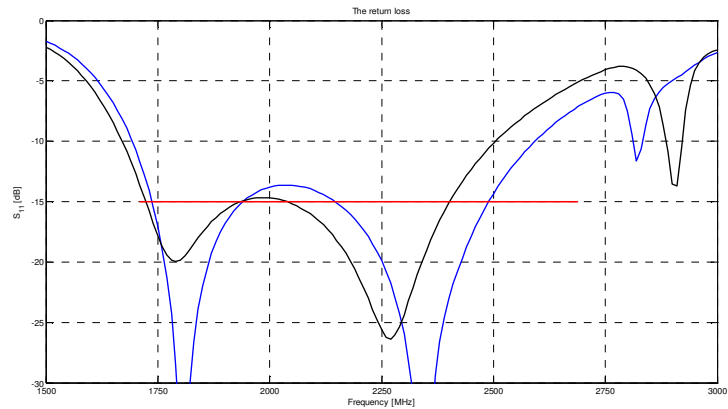


Figure 37: The return loss for the first antenna (blue curve) and for the second antenna (black curve).

	<i>Antenna 1</i>	<i>Antenna 2</i>
<i>Frequency band [MHz]</i>	1740-2490	1720-2400
<i>Fractional bandwidth</i>	35%	32%

Table 9: The bandwidth characteristics.

The radiation pattern can be seen in Figure 38. A concern is the ripple in the maximum gain for the highest frequency. The cross-polarization levels are below 15dB, and the back radiation is compressed more than 25dB compared to the maximum gain.

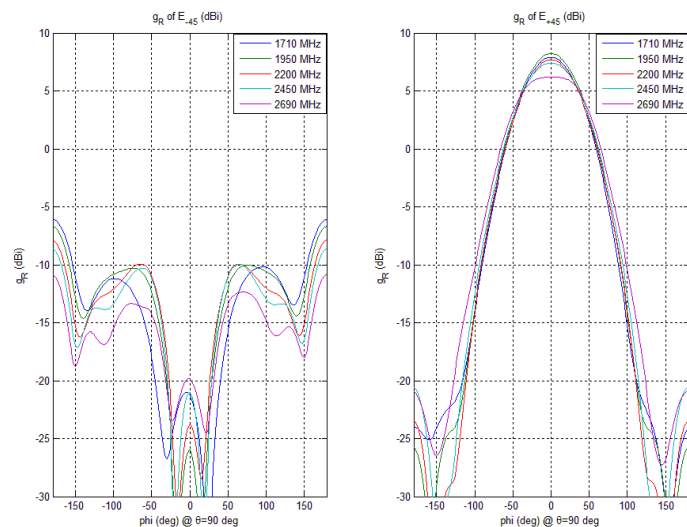


Figure 38: Horizontal radiation pattern ($\theta=90^\circ$) for the bowtie antenna.

The 3dB horizontal beamwidth was calculated for the five different frequencies (see Table 10).

Prepared (also subject responsible if other) EAB/FJN/AA Marie Ström		No. EAB/FJN-09:0218 Uen		
Approved EAB/FJN/A [Stefan Johansson]	Checked	Date 2009-07-02	Rev A	Reference

<i>Frequency [MHz]</i>	1710	1950	2200	2450	2690
<i>Beamwidth [Deg]</i>	87	81	81	95	100

Table 10: The 3dB horizontal beamwidth.

5.4 Detailed analysis for the printed dipole

Similar to the design for the bowtie antenna, the printed dipole is rotated +/- 45 degrees relative to the ground plane, and the size of the ground plane is changed to a square with dimensions 137x137mm. The S_{11} -parameters were exported from HFSS, and the theoretical matching properties given by the optimization in ADS can be seen in Figure 39. The return loss after optimizing is worse than 15dB. Hence, this design does not reach the requirement for the impedance bandwidth.

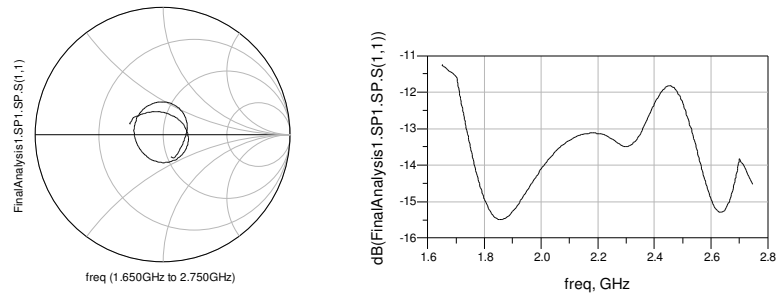


Figure 39: The Smith chart and the amplitude plot for the S_{11} -parameters for the printed dipole antenna optimized with ADS.

A way to improve the impedance matching could be to have an input impedance of 70Ω. The idea originates from the fact that a half wave dipole has a natural characteristic impedance of around 70Ω. The Marchand balun in ADS is instead optimized to the S_{11} -parameters with an antenna input impedance of 70Ω. Figure 40 shows the matching properties after the input impedance was changed. The result is a return loss that fulfills 15dB over the investigated frequency band.

Prepared (also subject responsible if other) EAB/FJN/AA Marie Ström		No. EAB/FJN-09:0218 Uen		
Approved EAB/FJN/A [Stefan Johansson]	Checked	Date 2009-07-02	Rev A	Reference

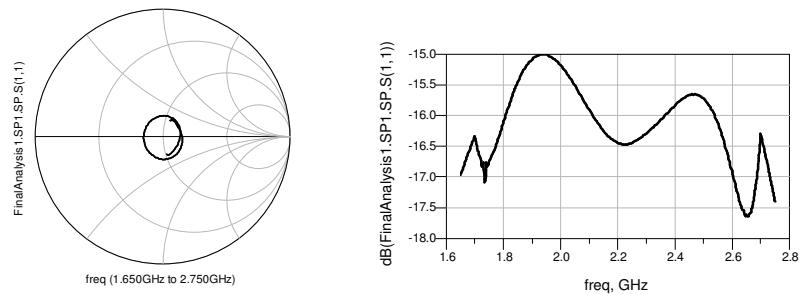


Figure 40: The Smith chart and the amplitude plot for the S_{11} -parameters for the printed dipole antenna optimized with ADS.

The optimized impedances and electrical lengths for the transmission lines are shown in Table 11.

Transmission line	Impedance [Ω]	Electrical length [θ]
Z_1	75	67
Z_b	57	78
Z_4	120	0
Z_{ab}	120	83

Table 11: Calculated impedances and electrical length for the printed dipole.

The impedances and electrical lengths were transformed to physical lengths and widths (see Table 12), using LineCalc in ADS for the microstrip lines.

Transmission line	Length [mm]	Width [mm]
Microstripline Z_1	16.7	1.01
Microstripline Z_b	19.3	1.6
CPS Z_4	0	0
CPS Z_{ab}	21.2	21.5

Table 12: The physical lengths and widths for the transmission lines.

To design the second polarization, Z_4 was tuned to have a physical length of 5mm. This makes it possible for the antennas to be mounted as a cross with low interference between each other. To compensate for the additional length of Z_4 , the length of Z_{ab} was tuned from 21.2mm to 32mm. The two printed dipole elements were mounted orthogonally with respect to each other, creating a cross (illustrated in Figure 41). When mounting the antennas together, there was no significant change in the matching properties.

Prepared (also subject responsible if other) EAB/FJN/AA Marie Ström		No. EAB/FJN-09:0218 Uen		
Approved EAB/FJN/A [Stefan Johansson]	Checked	Date 2009-07-02	Rev A	Reference

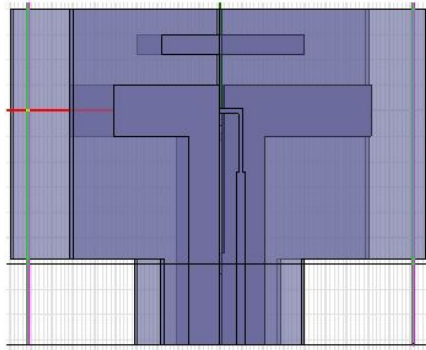


Figure 41: Two dipole antennas mounted in a cross to create a dual polarized antenna.

The matching properties for the dual polarized dipole antenna after an optimization are shown in Figure 42 and Figure 43, for the frequency range 1500 to 3000 MHz. The fractional bandwidth for the antenna was calculated in Matlab (see Table 13).

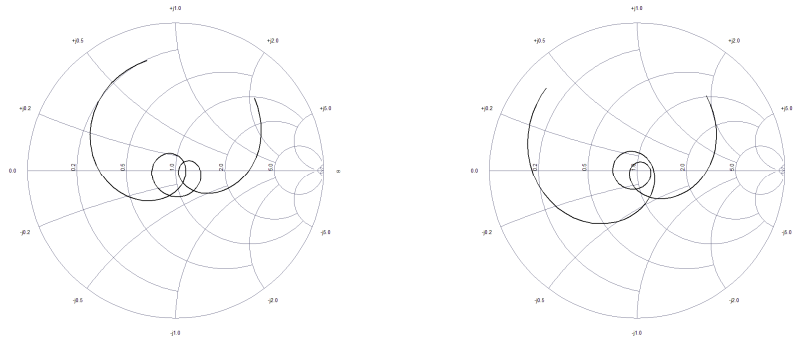


Figure 42: The Smith chart for the first antenna (to the left) and for the second antenna (to the right).

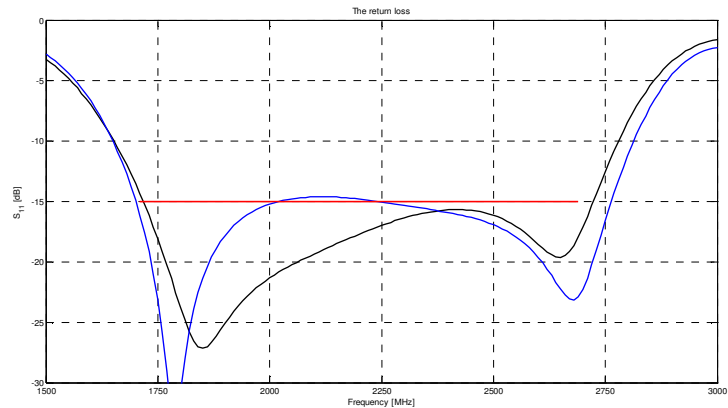


Figure 43: The return loss for the first antenna (blue curve) and for the second antenna (black curve).

Prepared (also subject responsible if other) EAB/FJN/AA Marie Ström		No. EAB/FJN-09:0218 Uen		
Approved EAB/FJN/A [Stefan Johansson]	Checked	Date 2009-07-02	Rev A	Reference

	<i>Antenna 1</i>	<i>Antenna 2</i>
<i>Frequency band [MHz]</i>	1690-2740	1710-2740
<i>Fractional bandwidth</i>	48.8%	47%

Table 13: The bandwidth characteristics.

The radiation pattern can be seen in Figure 44. The horizontal radiation pattern has a desirable shape, with low cross-polarization, side lobes and back radiation. However, there is a small ripple in the maximum gain between the lower and higher frequencies.

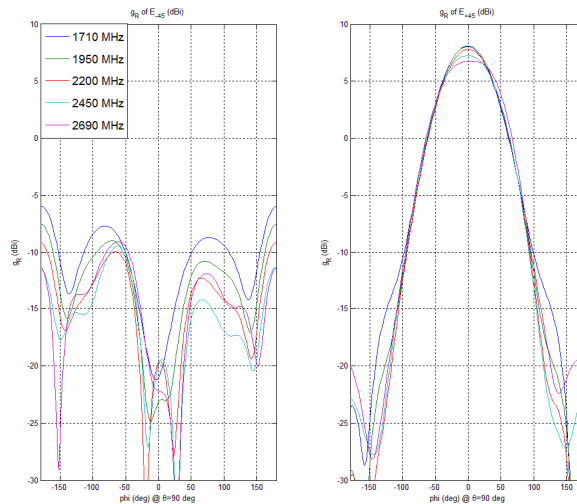


Figure 44: Horizontal radiation pattern ($\theta=90^\circ$) for the printed dipole.

To simulate how the antenna works in an array, boundary conditions were added in the z-plane and the dimensions of the ground plane were changed to 137x105mm. These changes result in a slightly worse matching for the lower frequencies. To compensate, the length of the radiator was changed from 68mm to 71mm. With this change the same bandwidth characteristic was achievable. However, there will be a change in the radiation pattern as seen in the left plot in Figure 45. The radiation pattern for the higher frequency has an undesirable appearance. To solve this problem, the *HGP* was changed from 33mm to 30mm and as seen in the right plot in Figure 45, a better result is achievable.

Prepared (also subject responsible if other) EAB/FJN/AA Marie Ström		No. EAB/FJN-09:0218 Uen		
Approved EAB/FJN/A [Stefan Johansson]	Checked	Date 2009-07-02	Rev A	Reference

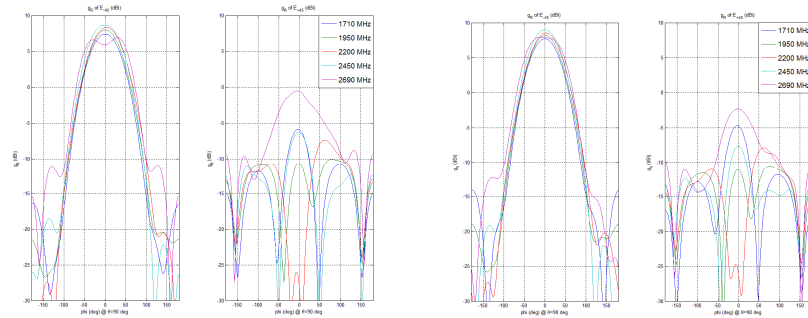


Figure 45: Radiation pattern after boundary conditions are added (to the left) and after changing *HGP* to 30mm (to the right).

The corresponding 3dB beamwidth (after the *HGP* was changed), was calculated in Matlab (see Table 14). The results are beamwidths between 70 to 80 degrees for the four lower frequencies and 90 degrees for the highest frequency. The detailed dimensions for the two antennas are presented in Table 15.

<i>Frequency [MHz]</i>	1710	1950	2200	2450	2690
<i>Beamwidth [Deg]</i>	73	73	74	75	90

Table 14: The 3dB horizontal beamwidth.

<i>Parameter</i>	L_{Dir}	W_{Dir}	L_{Par}	W_{Par}	S_{Par}	<i>HGP</i>	L_{Zab}
<i>Antenna 1 [mm]</i>	71	10	40	4	10	30	28
<i>Antenna 2 [mm]</i>	71	10	40	4	10	30	32
<i>Parameter</i>	L_{Z4}	W_{cps}	L_{Z1}	W_{Z1}	L_{Zb}	W_{Zb}	W_{Feed}
<i>Antenna 1 [mm]</i>	0	21.5	12.5	0.9	14	1.5	2
<i>Antenna 2 [mm]</i>	5	21.5	12.5	0.9	14	1.5	2

Table 15: Detailed dimensions for the two antennas.

Prepared (also subject responsible if other) EAB/FJN/AA Marie Ström		No. EAB/FJN-09:0218 Uen		
Approved EAB/FJN/A [Stefan Johansson]	Checked	Date 2009-07-02	Rev A	Reference

5.4.1 Removing the parasitic element

The parasitic strip was removed to evaluate how it affects the matching properties for the antenna. As can be seen in Figure 46, the return loss is worse for the higher frequencies, and in particular there is only one loop in the Smith chart. This implies that using a parasite improves the matching for the higher frequencies drastically.

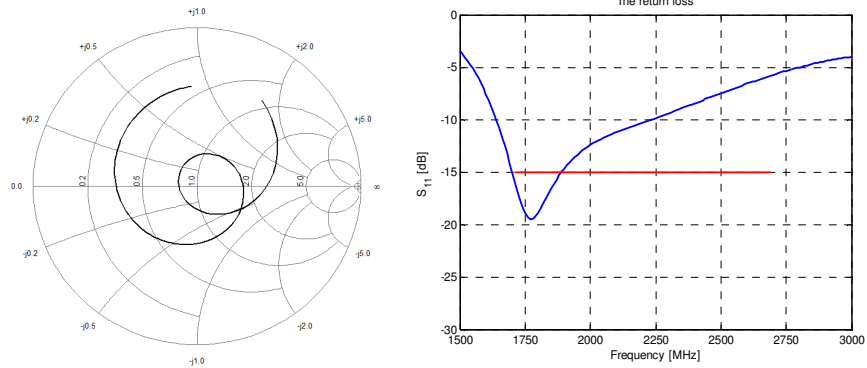


Figure 46: The Smith chart and the amplitude plot for the antenna without a parasitic element.

Prepared (also subject responsible if other) EAB/FJN/AA Marie Ström		No. EAB/FJN-09:0218 Uen		
Approved EAB/FJN/A [Stefan Johansson]	Checked	Date 2009-07-02	Rev A	Reference

6 Prototype manufacturing and measurements

The prototype was manufactured at Multi-Teknik in Göteborg. As a substrate, Neltec NX9300, with the same characteristics as Taconic RF-30, was used. Figure 47 and Figure 48 show the front and back side of the two antennas before being mounted together. The manufactured antenna is an earlier version and not the final layout. Hence, the result can only show if the matching properties are similar, worse, or better than the achieved result in HFSS.

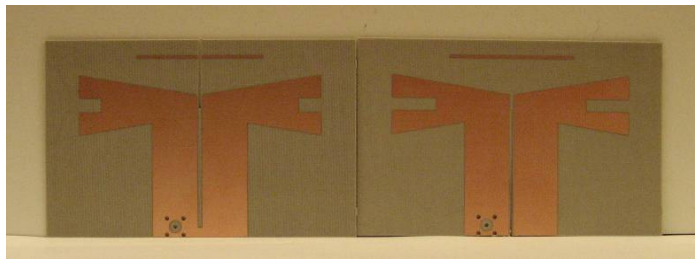


Figure 47: Front sides of the antenna prototype.

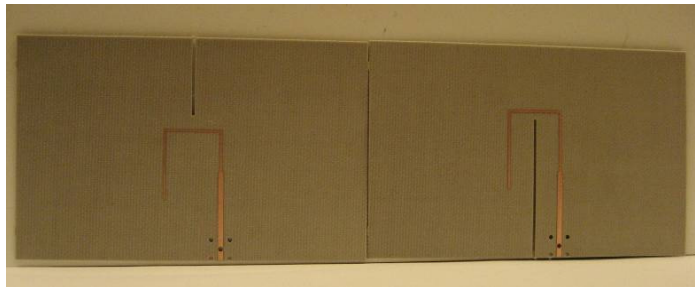


Figure 48: Back sides of the antenna prototype

As seen in Figure 47, the parasite for one antenna and the shorted CPS for the other antenna are not connected. Hence, after the antennas are mounted together, these parts have to be soldered to create a similar structure as in the simulations (see Figure 49).

Prepared (also subject responsible if other) EAB/FJN/AA Marie Ström		No. EAB/FJN-09:0218 Uen		
Approved EAB/FJN/A [Stefan Johansson]	Checked	Date 2009-07-02	Rev A	Reference

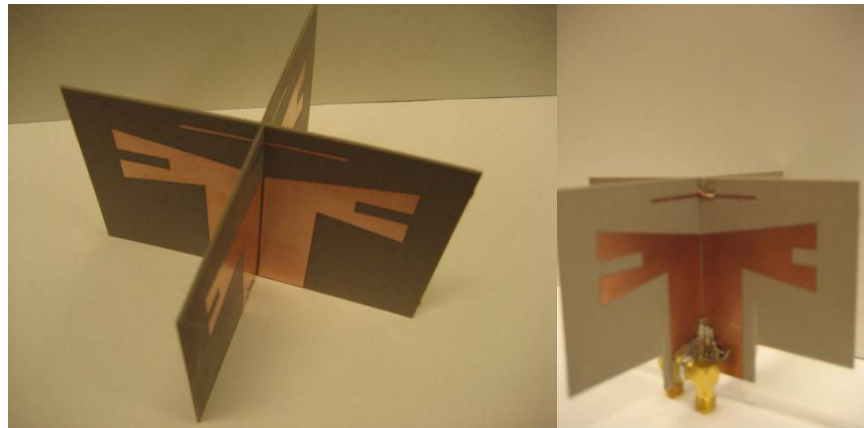


Figure 49: The antennas mounted together.

A 137mm wide metal sheet was used as a reflector, where two slots were cut out as a cross. The antenna was mounted on the reflector and connected to the network analyzer as seen in Figure 50.

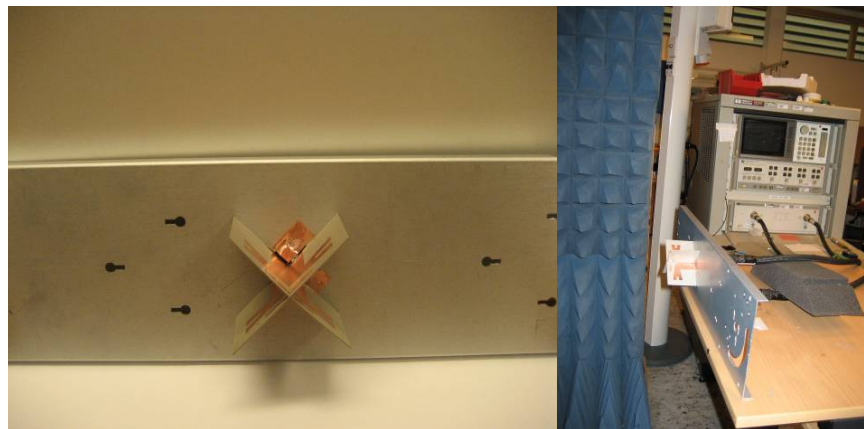


Figure 50: The antenna mounted on the reflector and the system setup.

The measurements were made in the antenna lab at Ericsson, Göteborg. To perform the measurements, an HP 8510 network analyzer calibrated at the interface of the coaxial cable for frequencies between 1.5 to 3 GHz was used. SMA connectors were attached to the antenna and connected to the network analyzer through two coaxial cables. The S-parameter matrices (S_{11} , S_{22} , S_{21} and S_{12}), were obtained and saved to a diskette as a *.cit file.

Prepared (also subject responsible if other) EAB/FJN/AA Marie Ström		No. EAB/FJN-09:0218 Uen		
Approved EAB/FJN/A [Stefan Johansson]	Checked	Date 2009-07-02	Rev A	Reference

6.1 Comparison between measurements and simulations

The matching properties for the prototype were imported to Matlab and compared with the simulations in HFSS (see Figure 51 and Figure 52). As can be seen, the return loss for both polarizations is better for the prototype compared with the simulations. The similarity between the S_{11} - and the S_{22} -plot implies that the results obtained in the simulations are consistent with the measurement for the prototype.

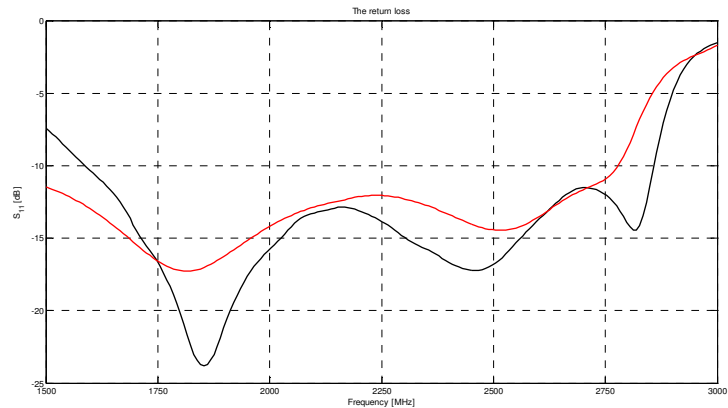


Figure 51: Comparison between the return loss (S_{11}) for the prototype (black curve) and the simulations (red curve).

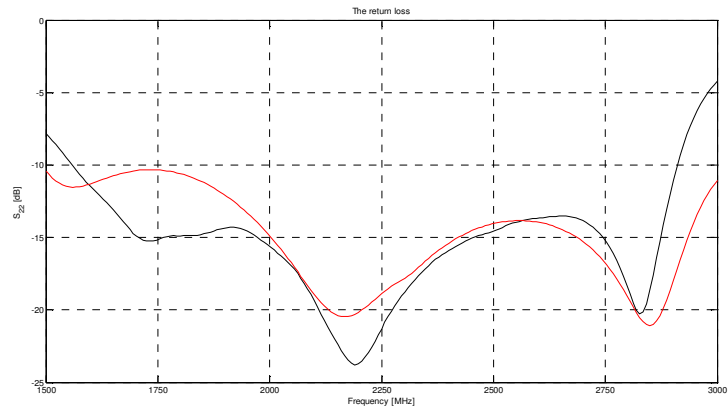


Figure 52: Comparison between the return loss (S_{22}) for the prototype (black curve) and the simulations (red curve).

Prepared (also subject responsible if other) EAB/FJN/AA Marie Ström		No. EAB/FJN-09:0218 Uen		
Approved EAB/FJN/A [Stefan Johansson]	Checked	Date 2009-07-02	Rev A	Reference

The amplitude plot of the S_{21} -parameters (see Figure 53), shows that the results obtained in HFSS are not similar to the measurements of the prototype. The isolation between the polarizations is better for the prototype compared with HFSS, for almost the entire frequency band. This may depend on the fact that, when simulating two wave ports in HFSS, the distance between the wave ports is too small and may cause mutual interference. The distance has to be this small due the fact that the dimension for a wave port has to be large enough to get the correct field behavior for a microstrip line.

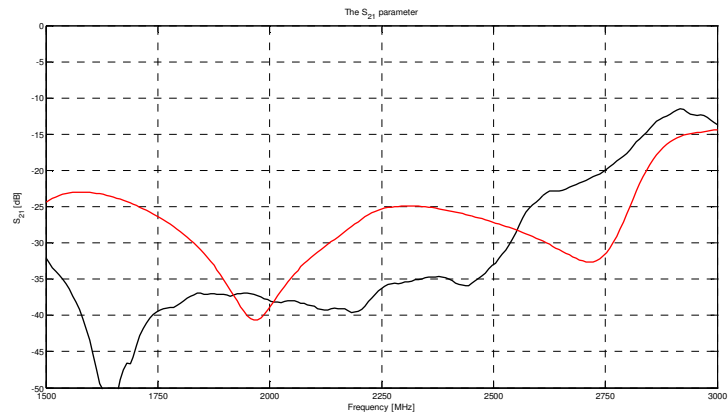


Figure 53: Comparison between the S_{21} -parameters for the prototype (black curve) and the simulations (red curve).

Figure 54 shows the Smith chart for the two antenna elements. It can be seen that closed loops are formed centered in the Smith chart, showing that the antenna is matched to an input impedance of 50Ω .

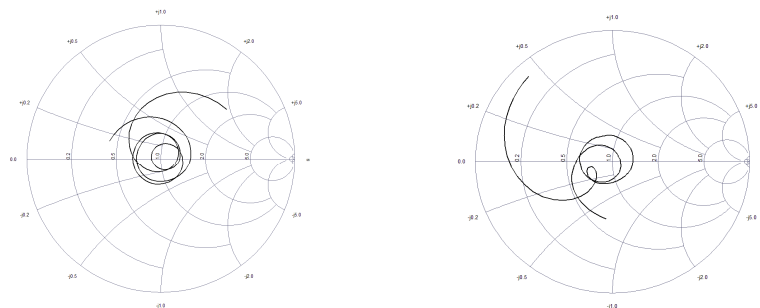


Figure 54: The Smith chart for the prototype, input 1 to the left and input 2 to the right.

Prepared (also subject responsible if other) EAB/FJN/AA Marie Ström		No. EAB/FJN-09:0218 Uen		
Approved EAB/FJN/A [Stefan Johansson]	Checked	Date 2009-07-02	Rev A	Reference

7 Discussion

The outcome of the literature study provided many interesting ideas. It appeared that both the printed dipole and the bowtie antenna with a parasitic strip would fulfill the requirements in terms of bandwidth. It was confirmed that, by adding the parasite, the matching properties for the high frequency band was enhanced. This contributes to an easier and better impedance matching for the entire frequency spectrum. However, a drawback is that by adding extra elements, the structure of the antenna becomes more complex and this can make the prototype manufacturing more difficult. The idea of adding a tuning slot, to achieve a better performance and to miniaturize the structure by increasing the electrical length of the bowtie was not fully examined. However, what can be seen is that, adding the tuning slot generates one more loop in the Smith chart, which can increase the frequency bandwidth. A concern is that when adding a large tuning slot, the radiation pattern is affected negatively.

To achieve dual polarization, mounting the antennas as a cross proves to be a good choice. This is mostly due to the fact that there is a low coupling between the antennas when mounted orthogonally to each other. Also, the additional slot in the substrate affects the antenna properties minimally.

In this project, the Marchand balun was used. An alternative could be to explore a different balun type. However, the Marchand balun is considered to be simple to implement and broadbanded. Furthermore, the other balun types appear to require too much space. The values of the balun parameters, which were optimized with ADS, are consistent with the results obtained for the same design in HFSS. Hence, the design of the balun is done comprehensively in ADS due to the fact that the optimization is much faster. Using a written Matlab script to calculate the correct width for the CPS gives an incorrect result, and this can be done better directly in HFSS.

A problem with the theoretical simulations is that the computational time in HFSS is high, and that the simulations sometimes finished with the error message "out of memory". A solution to this problem could be to write a script to connect HFSS with Matlab, and run the optimization in Matlab. However, in order to do that there is a need for more experience in HFSS.

The analysis of the matching properties for the prototype shows that the results are consistent with the simulations. One important difference is that there is less reflection losses in reality, compared with the simulations. Moreover, the mutual coupling is greater for the higher frequencies compared to the results from the simulations. This may depend on the difficulty to mount the antennas completely orthogonally to each other, and that a small change may affect the result drastically. After the antennas were mounted together, both the parasitic strip and the shorted CPS had to be soldered. This can cause an increased error, which may affect the coupling between the antennas.

Prepared (also subject responsible if other) EAB/FJN/AA Marie Ström		No. EAB/FJN-09:0218 Uen		
Approved EAB/FJN/A [Stefan Johansson]	Checked	Date 2009-07-02	Rev A	Reference

8 Conclusions

Comparisons of the matching properties for the two investigated concepts are shown in Table 16. Notable is that the matching for the two polarizations are highly independent of each other. The fractional bandwidth is greater for the printed dipole compared with the bowtie antenna.

Antenna 1	<i>Frequency band [MHz]</i>	<i>Fractional bandwidth</i>
<i>Printed dipole</i>	1690-2740	48.8%
<i>Bowtie</i>	1740-2490	35%
Antenna 2		
<i>Printed dipole</i>	1710-2740	47%
<i>Bowtie</i>	1720-2400	32%

Table 16: Comparison of the bandwidth between the printed dipole and the bowtie antenna.

Considering that the structure for the bowtie is more complex compared to the printed dipole; in particular there is an extra design parameter (L_{Imp}). Through further parameter optimization, it could be possible to achieve a better fractional bandwidth.

To enhance the impedance matching, the addition of a parasitic element gives an improved performance. This is necessary to accomplish the 15dB return loss criterion for entire frequency band.

For calculation of the transmission lines, ADS gives a similar result as HFSS and is therefore a good alternative due to the fast parameter optimization.

Examining the radiation pattern for the printed dipole shows that the 3dB beamwidth is larger than the requirements. However, a beamwidth up to 80 degrees is acceptable. A comparison between the 3dB beamwidth for the printed dipole and the bowtie antenna can be seen in Table 17.

<i>Frequency [MHz]</i>	<i>1710</i>	<i>1950</i>	<i>2200</i>	<i>2450</i>	<i>2690</i>
<i>Printed dipole</i>	73	73	74	75	90
<i>Bowtie</i>	87	81	81	95	100

Table 17: Comparison of the 3dB beamwidth between the printed dipole and the bowtie antenna.

The dimensions of the antenna element are 137x105x50mm, which fulfils the specific space requirement. Overall, the simulations show, that the printed dipole is preferable over the bowtie due to the fact that the matching characteristics, radiation pattern and 3dB beamwidth are better.

The prototype of a designed antenna was built and experimentally validated, showing a good agreement with the simulation result. Moreover, the matching properties for the prototype are better compared with the simulations.

Prepared (also subject responsible if other) EAB/FJN/AA Marie Ström		No. EAB/FJN-09:0218 Uen		
Approved EAB/FJN/A [Stefan Johansson]	Checked	Date 2009-07-02	Rev A	Reference

9 Proposed future work

To completely analyze the proposed antenna, a more detailed prototype has to be manufactured and evaluated in terms of return loss and radiation qualities. Moreover, to mount and analyze the antenna in an array would give knowledge about how the antenna behaves in an array environment.

In this report, it was not possible to fulfill the requirements, in terms of return loss and 3dB beamwidth with the bowtie antenna. However, through further optimization of the antenna parameters, it may be possible to accomplish the goals also with this concept.

One important improvement that could enhance the matching characteristics for the antenna is to compensate for the 90 degree bends in the balun. It is of importance that the bend is optimal in such a way that the incident wave is fully transmitted. A chamfered bend would reduce the parasitic effect for the capacitance.

An interesting solution to improve the performance for the antenna could be to add a second parasitic element below the radiator structure. The idea originates from the expected height of the antenna to the ground plane. A common rule of thumb is to mount the antenna half a wavelength over the ground plane. Hence, if the parasitic element is used to improve the performance for higher frequencies, it should to be placed closer to the ground plane. A second solution could be to instead optimize the radiator for the higher frequencies and the parasite for the lower frequencies. This would solve the problem of the expected distance between the element and the ground plane.

Prepared (also subject responsible if other) EAB/FJN/AA Marie Ström		No. EAB/FJN-09:0218 Uen		
Approved EAB/FJN/A [Stefan Johansson]	Checked	Date 2009-07-02	Rev A	Reference

10 References

- [1] IEEE Xplore:
<http://ieeexplore.ieee.org.proxy.lib.chalmers.se/Xplore/dynhome.jsp>
- [2] Engineering village:
<http://www.engineeringvillage2.org.proxy.lib.chalmers.se/controller/ser/vlet/Controller?CID=quickSearch&database=2>
- [3] Balanis, C. (1997) *Antenna theory: analysis and design*. 2nd Ed. John Wiley & Sons, Inc.
- [4] Costa, F. C. et al. (2006) *A New Quasi-Yagi Bowtie Type Integrated Antenna* in Telecommunications Symposium, 2006 International (2006) Fortaleza: Brazil. pp 468 – 471.
- [5] Zhou, Z. et al. (2007) *A Novel Broadband Printed Dipole Antenna With Low Cross-Polarization*. *IEEE transactions on antennas and propagation*, Vol. 55, No. 11, pp 3091-3096.
- [6] Lu, X. P. & Li, Y. (2006) *Novel broadband printed dipole*. *Microwave and optical technology letters*, Vol. 48, No. 10, pp 1996-1998.
- [7] Marantis, L. & Brennan, P. (2008) *A CPW-fed Bow-tie slot antenna with tuning stub* in Loughborough Antenna & Propagation Conference. Antennas and Propagation Conference, 2008. LAPC 2008. Loughborough, pp 389 – 392.
- [8] Anantapreecha, W. et al. (2007) *Novel E-Shaped Driver based on the Quasi-Yagi Antenna* in the 9th International Conference. Advanced Communication Technology, The 9th International Conference 2007, pp 894 – 896.
- [9] Ansari, J. A. et al. (2008) *Analysis of Stacked V-Slot Loaded Patch Antenna for Wideband Application*. *Microwave and optical technology letters*, Vol. 51, No. 2, pp 324-330.
- [10] Ghorbani, K. & Waterhouse, R. B. (2004) *Dual polarized wide-band aperturestacked patch antennas*. *IEEE transactions on antennas and propagation*, Vol. 52, No. 2, pp 2171-2174.
- [11] Guo, Y. X., Khoo, K.-W. & Ong, L. C. (2007) *Wideband Dual-Polarized Patch Antenna with Broadband Baluns*. *IEEE transactions on antennas and propagation*, Vol. 55, No. 1, pp 78-83.
- [12] Miron, Douglas B. (2006) *Small antenna design*. Elsevier Inc.
- [13] Karlsson, H. (1997) *Dual-polarized omnidirectional antenna*. Master thesis at Ericsson Microwaves. Mölndal, Sweden
- [14] Losee, Ferril A. (2005) *RF Systems, components, and circuits handbook*. 2nd Ed. Artech house, Inc.

Prepared (also subject responsible if other) EAB/FJN/AA Marie Ström		No. EAB/FJN-09:0218 Uen		
Approved EAB/FJN/A [Stefan Johansson]	Checked	Date 2009-07-02	Rev A	Reference

- [15] Grosch, Theodore (1999) *Small Signal Microwave Amplifier Design*. Noble Publishing Corporation.
- [16] Cheng, David K. (1989) *Field and Wave Electromagnetics*. 2nd Ed. Addison-Wesley Publishing Company, Inc.
- [17] Volakis, J. L. (2007) *Antenna engineering handbook*. 4th Ed. McGraw-Hill.
- [18] Ansoft, *Simulation Software for high performance electronic design*. <http://www.ansoft.com/> [viewed 02/04/2009].
- [19] Agilent Technologies: <http://www.home.agilent.com/agilent/home.jsp> [viewed 02/04/2009]
- [20] The Mathworks, *Matlab and simulink for technical computation*. <http://www.mathworks.com/> [viewed 02/04/2009]
- [21] Kompa, Günter (2005) *Practical Microstrip Design and Applications*. Artech house, Inc.
- [22] Wadell, B. C. (1991) *Transmission Line Design Handbook*. Artech house, Inc. London & Boston

Prepared (also subject responsible if other) EAB/FJN/AA Marie Ström		No. EAB/FJN-09:0218 Uen		
Approved EAB/FJN/A [Stefan Johansson]	Checked	Date 2009-07-02	Rev A	Reference

Appendix A: Formulas

Microstrip line

Figure 55 shows the design of the microstrip line.

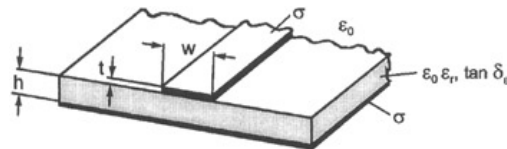


Figure 55: Microstrip line [21]

Below, the formulas to calculate the characteristic impedance Z_0 and the effective dielectric constant $\epsilon_{eff} = \epsilon_0 \epsilon_r$ are shown.

$$Z_0 = \frac{\eta_0}{2\sqrt{2\pi}\sqrt{\epsilon_{eff} + 1}} \ln \left\{ 1 + \frac{4h}{w'} \left[\frac{1 + \frac{8}{\epsilon_{eff}}}{11} \frac{4h}{w'} + \sqrt{\frac{14 + \frac{1}{\epsilon_{eff}}}{2} \pi^2} \right] \right\} \quad \text{Eq. 7}$$

If, $\frac{w}{h} \leq 1$:

$$\epsilon_{eff} = \frac{\epsilon_r + 1}{2} + \frac{\epsilon_r - 1}{2} \left[\left(1 + \frac{12h}{w} \right)^{-0.5} + 0.04 \left(1 - \frac{w}{h} \right)^2 \right] \quad \text{Eq. 8}$$

If, $\frac{w}{h} > 1$:

$$\epsilon_{eff} = \frac{\epsilon_r + 1}{2} + \frac{\epsilon_r - 1}{2} \left(1 + \frac{12h}{w} \right)^{-0.5} \quad \text{Eq. 9}$$

The height of the substrate is taken into account by introducing an equivalent change in the width for the line wire (Δw). This is described by the following formulas.

Prepared (also subject responsible if other) EAB/FJN/AA Marie Ström		No. EAB/FJN-09:0218 Uen		
Approved EAB/FJN/A [Stefan Johansson]	Checked	Date 2009-07-02	Rev A	Reference

$$\frac{\Delta w}{t} = \frac{1}{\pi} \ln \left[\frac{4e}{\sqrt{\left(\frac{t}{h}\right)^2 + \left(\frac{1/\pi}{w/t + 1.1}\right)^2}} \right] \quad \text{Eq. 10}$$

$$\Delta w' = \Delta w \left(\frac{1 + 1/\epsilon_r}{2} \right)$$

$$w' = w + \Delta w'$$

The ground plane can be seen as infinite for the microstrip line, if the width of it is at least three times greater than the width of the microstrip line. When this rule of thumb is satisfied, the uncertainty is less than 3% for Z_0 and even smaller for ϵ_{eff} [21].

Coplanar stripline

The CPS design can be seen in Figure 56.

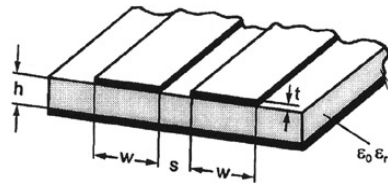


Figure 56: Coplanar stripline [21]

The characteristic impedance for a CPS is calculated with Eq. 11.

$$Z_0 = \frac{\eta_0}{\sqrt{\epsilon_{eff}}} \frac{K(k)}{K(k')} \quad \text{Eq. 11}$$

Where the wave impedance $\eta_0 = 120\pi$ and $K(k)$ is the first order complete elliptic integral. The constant ϵ_{eff} is calculated with Eq. 12, Eq. 13, Eq. 14, Eq. 15 and Eq. 16.

$$\epsilon_{eff} = 1 + \frac{\epsilon_r - 1}{2} \frac{K(k')K(k_1)}{K(k)K(k_1')} \quad \text{Eq. 12}$$

Prepared (also subject responsible if other) EAB/FJN/AA Marie Ström		No. EAB/FJN-09:0218 Uen		
Approved EAB/FJN/A [Stefan Johansson]	Checked	Date 2009-07-02	Rev A	Reference

$$k = \frac{a}{b} \quad \text{Eq. 13}$$

$$k_1 = \frac{\sinh\left(\frac{\pi a}{4h}\right)}{\sinh\left(\frac{\pi b}{4h}\right)} \quad \text{Eq. 14}$$

$$k' = \sqrt{1 - k^2} \quad \text{Eq. 15}$$

$$k_1' = \sqrt{1 - k_1^2} \quad \text{Eq. 16}$$

Marchand balun of the fourth order (formulas from [13])

Assume that all the transitions are lossless and that there is no dispersion in the transmission lines.

The reflection coefficient is calculated as:

$$|\rho|^2 = \frac{[\varepsilon Mch_n(\theta, \theta_c)]^2}{1 + [\varepsilon Mch_n(\theta, \theta_c)]^2}$$

$$Mch_n(\theta, \theta_c) = T_2\left(\frac{\tan \theta_c}{\tan \theta}\right) T_{n-2}\left(\frac{\cos \theta}{\cos \theta_c}\right) - U_2\left(\frac{\tan \theta_c}{\tan \theta}\right) U_{n-2}\left(\frac{\cos \theta}{\cos \theta_c}\right)$$

Where $n=4$, for the fourth order balun, θ is the electrical length of the transmission line. When the physical length of the transmission line is $l = \frac{\lambda_g}{4}$ at the center of the pass band, θ_c can be expressed as:

$$\theta_c = \frac{\pi}{B + 1}$$

Where,

$$B = \frac{f_{upper}}{f_{lower}}$$

The first order Chebyshev polynomial is defined as:

$$T_{n-2}(x) = \cos((n-2) \arccos(x)),$$

The second order Chebyshev polynomial is defined as

Prepared (also subject responsible if other) EAB/FJN/AA Marie Ström		No. EAB/FJN-09:0218 Uen		
Approved EAB/FJN/A [Stefan Johansson]	Checked	Date 2009-07-02	Rev A	Reference

$$U_{n-2}(x) = \sin((n-2) \arccos(x))$$

The specific equations to solve the impedances for the fourth order balun are seen below.

$$r_{i1} = z_1^2 \frac{1 + \tan^2 \theta}{z_1^2 + \tan^2 \theta}$$

$$x_{i1} = z_1 \tan \theta \frac{z_1^2 - 1}{z_1^2 + \tan^2 \theta}$$

$$r_{i4} = z_4^2 r \frac{1 + \tan^2 \theta}{z_4^2 + r^2 \tan^2 \theta}$$

$$x_{i4} = z_4 \tan \theta \frac{z_4^2 - r^2}{z_4^2 + r^2 \tan^2 \theta}$$

$$r_{in}^e = \frac{r_{i4} z_{ab}^2 \tan^2 \theta}{r_{i4}^2 + (x_{i4} + z_{ab} \tan \theta)^2}$$

Prepared (also subject responsible if other) EAB/FJN/AA Marie Ström		No. EAB/FJN-09:0218 Uen		
Approved EAB/FJN/A [Stefan Johansson]	Checked	Date 2009-07-02	Rev A	Reference

Appendix B: Radiation pattern for various designs

Basic design parameters for the bowtie radiator

Number	HGP [mm]	L_{Bow} [mm]
1	46	60
2	46	70
3	46	80
4	30	60
5	30	70
6	30	80

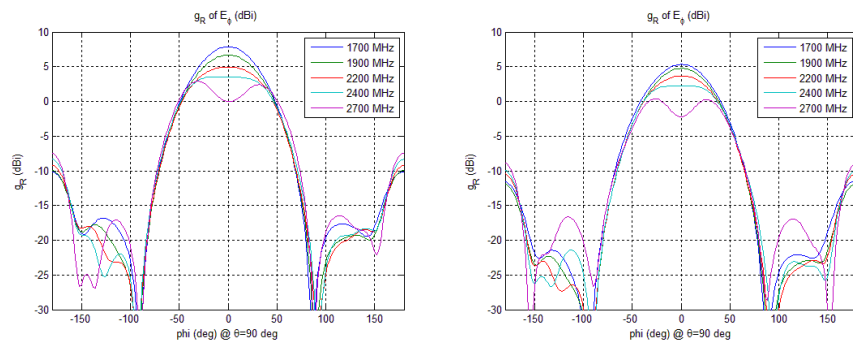


Figure 57: Number 1 (to the left) and Number 2 (to the right).

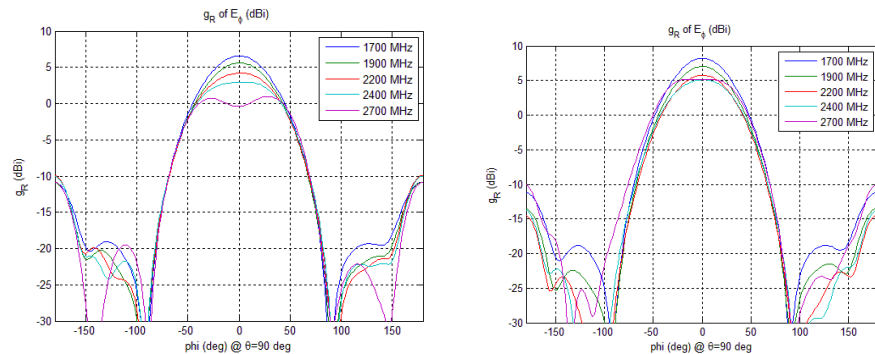


Figure 58: Number 3 (to the left) and Number 4 (to the right).

Prepared (also subject responsible if other) EAB/FJN/AA Marie Ström		No. EAB/FJN-09:0218 Uen		
Approved EAB/FJN/A [Stefan Johansson]	Checked	Date 2009-07-02	Rev A	Reference

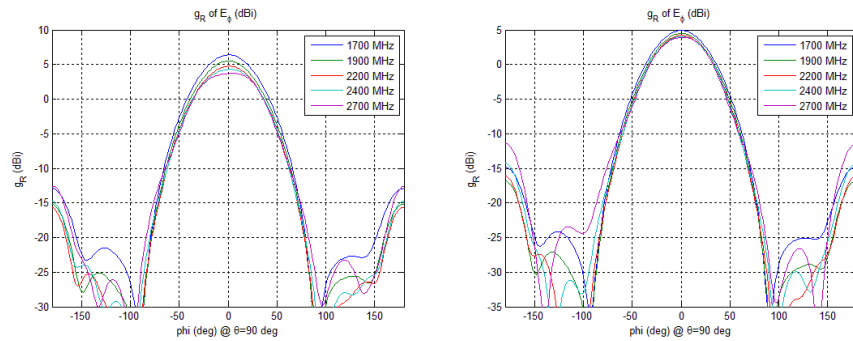


Figure 59: Number 5 (to the left) and Number 6 (to the right).

Change of values for the parasitic element

Number	L_{Bow} [mm]	L_{Par} [mm]	S_{Par} [mm]
4	80	37	8.8
5	80	55	8.8
6	80	55	15
7	80	45	15
8	80	37	15
9	80	37	10

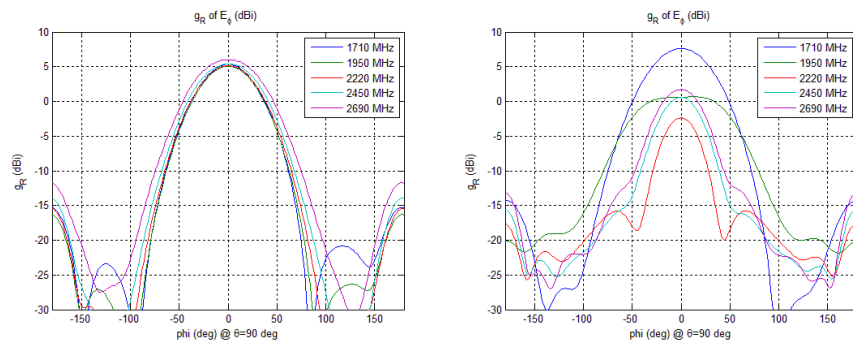


Figure 60: Number 4 (to the left) and Number 5 (to the right).

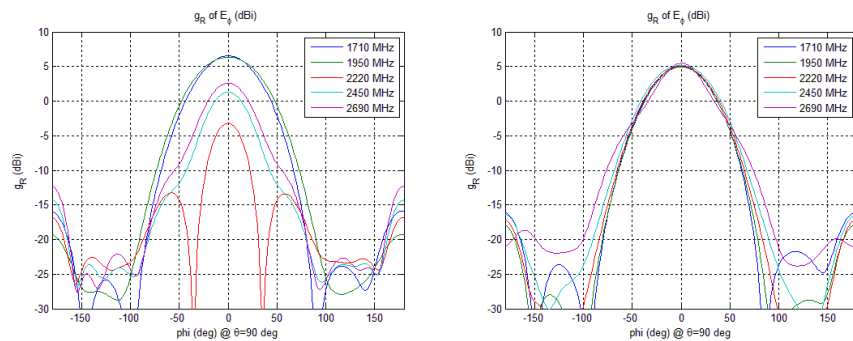


Figure 61: Number 6 (to the left) and Number 7 (to the right).

Prepared (also subject responsible if other) EAB/FJN/AA Marie Ström		No. EAB/FJN-09:0218 Uen		
Approved EAB/FJN/A [Stefan Johansson]	Checked	Date 2009-07-02	Rev A	Reference

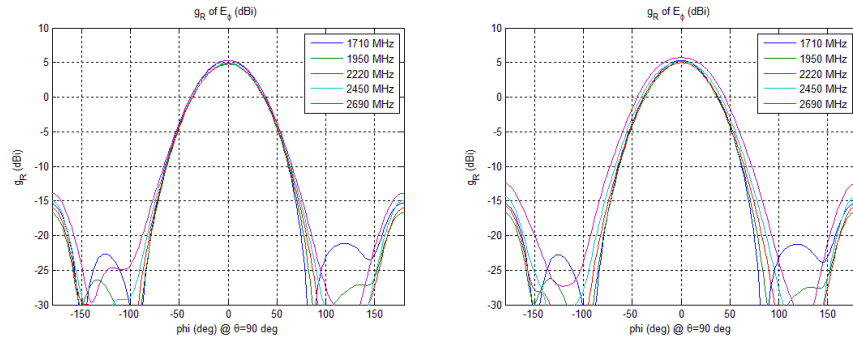


Figure 62: Number 8 (to the left) and Number 9 (to the right).

Change of length for the tuning slot

Number	L_{Bow} [mm]	L_{Slot} [mm]
12	60	23
13	80	23
14	80	10
15	80	30

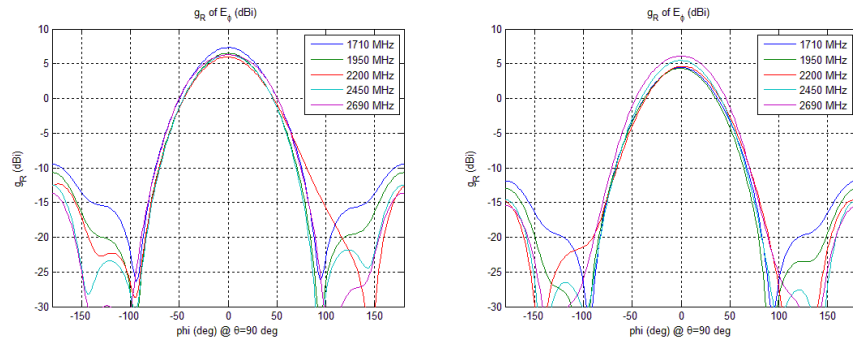


Figure 63: Number 12 (to the left) and Number 13 (to the right).

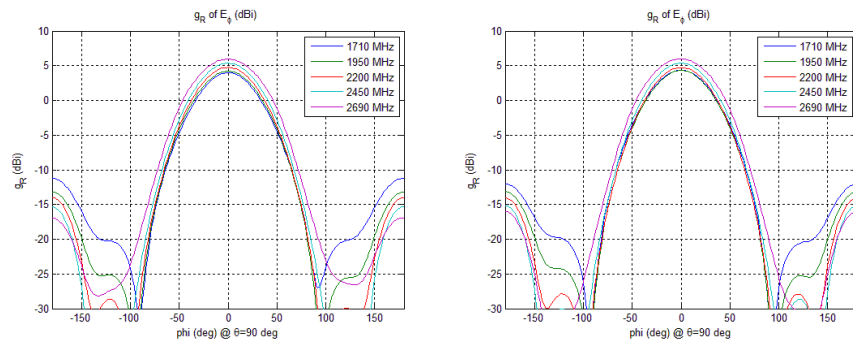


Figure 64: Number 14 (to the left) and Number 15 (to the right).